2016-10-04

Ataluren stimulates ribosomal selection of near-cognate tRNAs to promote nonsense suppression

Bijoyita Roy
University of Massachusetts Medical School

Et al.

Ataluren stimulates ribosomal selection of near-cognate tRNAs to promote nonsense suppression

Bijoyita Roy[a,b,1], Westley J. Friesen[b,1], Yuki Tomizawa[b], John D. Leszyk[c], Jin Zhuo[b], Briana Johnson[b], Jumana Dakka[b], Christopher R. Trotta[b], Xiaojiao Xue[b,d,e], Venkateshwar Mutyam[e,f], Kim M. Keeling[d,e], James A. Mobley[g], Steven M. Rowe[e,f], David M. Bedwell[d,e], Ellen M. Welch[b], and Allan Jacobson[a,2]

[a]Department of Microbiology and Physiological Systems, University of Massachusetts Medical School, Worcester, MA 01655-0122; [b]PTC Therapeutics Inc., South Plainfield, NJ 07080; [c]Department of Biochemistry and Molecular Pharmacology, University of Massachusetts Medical School, Worcester, MA 01655-0122; [d]Department of Biochemistry and Molecular Genetics, University of Alabama at Birmingham, Birmingham, AL 35294; [e]Gregory Fleming James Cystic Fibrosis Research Center, University of Alabama at Birmingham, Birmingham, AL 35294; [f]Department of Medicine, University of Alabama at Birmingham, Birmingham, AL 35294; and [g]Department of Surgery, University of Alabama at Birmingham, Birmingham, AL 35294

Edited by Rachel Green, Johns Hopkins University, Baltimore, MD, and approved September 6, 2016 (received for review April 1, 2016)

A premature termination codon (PTC) in the ORF of an mRNA generally leads to production of a truncated polypeptide, accelerated degradation of the mRNA, and depression of overall mRNA expression. Accordingly, nonsense mutations cause some of the most severe forms of inherited disorders. The small-molecule drug ataluren promotes therapeutic nonsense suppression and has been thought to mediate the insertion of near-cognate tRNAs at PTCs. However, direct evidence for this activity has been lacking. Here, we expressed multiple nonsense mutation reporters in human cells and yeast and identified the amino acids inserted when a PTC occupies the ribosomal A site in control, ataluren-treated, and aminoglycoside-treated cells. We find that ataluren's likely target is the ribosome and that it produces full-length protein by promoting insertion of near-cognate tRNAs at the site of the nonsense codon without apparent effects on transcription, mRNA processing, mRNA stability, or protein stability. The resulting readthrough proteins retain function and contain amino acid replacements similar to those derived from endogenous readthrough, namely Gln, Lys, or Tyr at UAA or UAG PTCs and Trp, Arg, or Cys at UGA PTCs. These insertion biases arise primarily from mRNA:tRNA mispairing at codon positions 1 and 3 and reflect, in part, the preferred use of certain nonstandard base pairs, e.g., U-G. Ataluren's retention of similar specificity of near-cognate tRNA insertion as occurs endogenously has important implications for its general use in therapeutic nonsense suppression.

nonsense suppression | readthrough | Translarna | base mispairing

Nonsense mutations are responsible for ∼10–15% of the single-base-pair mutations that cause human disease, with some disease genes having considerably higher nonsense mutation frequencies (1). Patients with genetic disorders attributable to nonsense mutations tend to have more serious ramifications than those with missense mutations, presumably because of marked reductions in specific gene expression. Because all diseases caused by nonsense mutations share the same key gene expression problems, namely premature translation termination and accelerated mRNA decay, therapeutic approaches to these problems are being investigated, with the understanding that a single drug has the potential to treat a large number of different disorders (1, 2). Normally, the in-frame UAG, UAA, and UGA codons that arise in mRNA from nonsense mutations serve as signals for translation termination, but this role can be functionally overridden by alterations in the translation machinery or by the presence of certain small molecules that compromise the fidelity of translation termination (1, 2). Such nonsense suppression, or nonsense codon readthrough, by a ribosome engaged in peptide elongation has been predominantly observed in the context of premature termination codons (PTCs) and is thought to reflect ribosomal A site acceptance of a near-cognate tRNA and subsequent incorporation of an amino acid into the nascent polypeptide at the position of the PTC (1, 2).

The small-molecule drug ataluren (3-[5-(2-fluorophenyl)-1,2,4-oxadiazol-3-yl]-benzoic acid; also known as Translarna or PTC124) is being evaluated both preclinically and clinically for its ability to promote therapeutic nonsense suppression (1, 3). To date, ataluren has been shown to restore function to more than 20 different disease-specific or reporter nonsense alleles in systems ranging in complexity from in vitro translation to cell culture to mouse models and human patients (1, 3–14). In the latter, Translarna clinical trials have demonstrated restoration of full-length functional protein in Duchenne muscular dystrophy and cystic fibrosis nonsense mutation patients (10, 11, 13, 15, 16). However, a lack of activity has been reported for some cell systems (17, 18).

Here, we have investigated the mechanistic basis of PTC readthrough induced by ataluren in human and yeast cells and compared it to the activity of two other readthrough-promoting compounds, the aminoglycosides G418 and gentamicin. Using multiple reporters and a physiologically relevant *CFTR* (cystic fibrosis transmembrane conductance regulator) nonsense allele, we have determined the nature of the translation events at PTCs when cells are treated with these drugs. Our study provides comprehensive characterization of the products of PTC readthrough and elucidates the nature of the nonstandard codon:anticodon base pairings that are favored under physiological conditions in the cell. These proof-of-concept

Significance

The drug ataluren restores activity to otherwise nonfunctional nonsense alleles, a capability possibly reflecting the insertion of near-cognate aminoacyl tRNAs at premature termination codons during protein synthesis. Because nonsense alleles comprise a significant fraction of all alleles causing inherited disorders, drugs that promote such nonsense codon readthrough have broad therapeutic potential. However, the effectiveness of therapeutic nonsense suppression depends on the nature of the amino acids inserted at each of the three nonsense codons. Here we demonstrate that ataluren does indeed promote insertion of near-cognate tRNAs at nonsense codons, that the latter process yields functional proteins, and that specific codon:anticodon base pairings are critical to this process. These results should enable predictions of better clinical outcomes with therapeutic nonsense suppression.

Author contributions: B.R., W.J.F., K.M.K., D.M.B., E.M.W., and A.J. designed research; B.R., W.J.F., Y.T., J.D.L., J.Z., B.J., J.D., C.R.T., X.X., V.M., and K.M.K. performed research; B.R., W.J.F., J.D.L., K.M.K., J.A.M., S.M.R., D.M.B., E.M.W., and A.J. analyzed data; and B.R., W.J.F., and A.J. wrote the paper.

Conflict of interest statement: B.R., W.J.F., Y.T., J.Z., B.J., J.D., C.R.T., X.X., and E.M.W. are employees of PTC Therapeutics Inc. (PTCT). A.J. is a cofounder, director, and consultant for PTCT, and D.M.B. is a consultant for PTCT. S.M.R. receives grant support from PTCT to conduct clinical trials for the treatment of cystic fibrosis.

This article is a PNAS Direct Submission.

Freely available online through the PNAS open access option.

[1]B.R. and W.J.F. contributed equally to this work.

[2]To whom correspondence should be addressed. Email: allan.jacobson@umassmed.edu.

This article contains supporting information online at www.pnas.org/lookup/suppl/doi:10.1073/pnas.1605336113/-/DCSupplemental.

experiments establish unambiguously that these compounds promote insertion of near-cognate tRNAs at PTCs and provide insight into the likelihood of functionality for the products of therapeutic nonsense suppression.

Results

Ataluren Promotes Nonsense Suppression in Mammalian Cells and Yeast. Six different PTC reporter genes, including some with multiple alleles, were used to monitor different aspects of nonsense codon readthrough in human cells and yeast (*SI Appendix*, Fig. S1). PTC-containing transcripts arising from selected reporters are substrates for nonsense-mediated mRNA decay (*SI Appendix*, Fig. S2). Ataluren treatment of mammalian 293H cells stably transfected with wild-type (WT) or PTC(W12X)-containing NanoLuc (19) reporters promoted a bell-shaped dose–response, with a peak ninefold increase in luciferase activity derived from the PTC reporter at 10 μM (Fig. 1). This result was attributable to readthrough of the reporter mRNA's premature UGA codon, and not protein stabilization (18), because ataluren treatment of 293H cells stably expressing WT NanoLuc had no effect on NanoLuc activity (Fig. 1*B*). In *SI Appendix*, Fig. S3 *A* and *B* demonstrate that ataluren (and G418) also promote readthrough of different p53 UGA alleles in Calu6 and HDQ cells and of a UGA PTC in an H2B-GFP reporter (6) expressed in 293H cells.

Yeast WT [*PSI*−] cells devoid of the prion form of Sup35 (to ensure that the readthrough observed was solely attributable to drug treatment) showed ataluren-dependent increases in readthrough from the HA-*HIS3*$_{(UAA100)}$-SF or HA-*LUC*$_{(UGA20)}$-SF reporter mRNAs without concomitant changes in mRNA levels albeit at higher concentrations than used for mammalian cells, a difference probably attributable to the yeast cell membrane (Fig. 1*C*; *SI Appendix*, Figs. S2 *A* and *B* and S4). This indicated that ataluren treatment directly affected reporter protein abundance, not alterations in transcription, mRNA processing, or mRNA stability. In cycloheximide chase assays, ataluren treatment also did not change the half-life of the full-length His3 readthrough protein, indicating that the drug affects PTC readthrough per se (*SI Appendix*, Fig. S5). Consistent with this conclusion, the prematurely terminated His3 polypeptide fragment that is detectable only by its N-terminal tag in *upf1Δ* cells (20) decreases in abundance as synthesis of the full-length His3 product increases (Fig. 1*C*, *Top*; see "His3 PTC" in DMSO and ataluren lanes in *upf1Δ* cells).

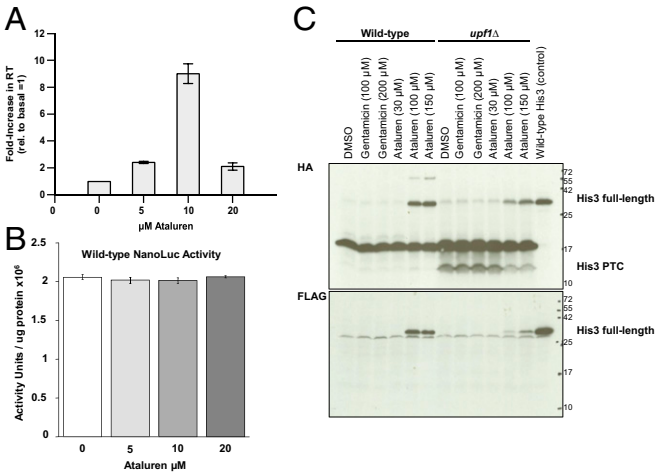

Fig. 1. Ataluren treatment of mammalian or yeast cells increases PTC readthrough. Dose–response of ataluren treatment in 293H cells stably transfected with (*A*) PTC(UGA$_{W12X}$) or (*B*) wild-type (WT) NanoLuc reporters. The 293H cells stably expressing the NanoLuc reporters were treated with ataluren at the indicated concentrations. The data are expressed as the mean ± SD of the NanoLuc activity units normalized to total protein. (*C*) Western analyses of yeast cells showing readthrough products expressed from HA-*HIS3*$_{(UAA100)}$-SF reporters after ataluren or gentamicin treatment. *Upper* and *Lower* blots, respectively, were probed for the HA (N-terminal) and FLAG (C-terminal) epitopes. The predominant band at ∼17 kDa in the HA blot is an HA artifact detected only in cells expressing *HIS3*$_{(UAA100)}$-SF, but not *HIS3*$_{(WT)}$-SF.

Near-Cognate tRNAs Facilitate Ataluren-Mediated Readthrough. We identified the amino acids inserted at PTCs in drug-treated cells using a firefly luciferase (*LUC*) reporter system that yields highly purified readthrough products and well-resolved peptides suitable for mass spectrometry and amino acid sequence determination (*SI Appendix*, Fig. S1*C*) (21). It has been suggested that ataluren is an inhibitor of firefly luciferase and that its reported nonsense suppression activity simply reflects stabilization of the luciferase enzyme (18, 22). We consider this claim to be spurious because (*i*) ataluren-mediated readthrough has been observed in numerous other systems (Fig. 1 and *SI Appendix*, Fig. S3) (1–14, 23); (*ii*) the effects on luciferase activity could not be independently replicated by others (24) or by us (*SI Appendix*, Fig. S3*C*); (*iii*) ataluren's putative luciferase inhibitory activity depends on a specific enzyme substrate (25); and (*iv*) most of the hypothetical inhibitory molecule, PTC124-AMP (22), is rapidly converted to the active readthrough molecule PTC124 (ataluren) under conditions of in vitro translation (*SI Appendix*, Fig. S6). Accordingly, three of the HA-*LUC*$_{(PTC20)}$-SF reporters were separately expressed in yeast WT [*PSI*−] cells. Strep-Tactin purification of the respective readthrough products synthesized in the absence or presence of ataluren was monitored by gel electrophoresis to resolve full-length proteins (*SI Appendix*, Fig. S7). Following silver staining of the gel, the band corresponding to full-length luciferase protein was excised and subjected to endo-LysC digestion and LC-MS/MS analysis, and amino acid insertion frequencies were determined as described previously (21). Analysis of the readthrough products purified from untreated cells showed the incorporation of Gln, Lys, and Tyr at UAA and UAG and insertion of Trp, Arg, and Cys at UGA, all of which were similar to results reported previously for endogenous background readthrough (Fig. 2*A*) (21, 26). Readthrough products purified from cells treated with ataluren showed that Gln, Lys, and Tyr were also inserted when UAA was the PTC (Fig. 2*A*). Three independent experiments revealed that the frequencies of insertion of Tyr and Gln were comparable (51.5 ± 2% and 46.4 ± 2%, respectively) and that Lys was inserted at a much lower frequency (2 ± 1.7%) (Fig. 2*A*). Readthrough from UAG resulted in the insertion of the same sets of amino acids, but with different frequencies. Gln insertion predominated, with a frequency of 88 ± 3.6%, whereas Tyr (8.6 ± 2%) and Lys (3.3 ± 1.5%) had somewhat similar insertion frequencies (Fig. 2*A*). With UGA as the PTC, ataluren treatment resulted in the incorporation of Trp, Arg, and Cys, with Trp insertions occurring at a much higher frequency (86.3 ± 3%) than those of Arg (4.6 ± 2%) or Cys (9 ± 2%) (Fig. 2*A*). A comparison of the endogenous readthrough events with those mediated by ataluren indicates that there are no major differences in the respective amino acid insertion frequencies in yeast cells.

In contrast to the results obtained when readthrough was promoted by ataluren, treatment of [*PSI*−] yeast cells with 7.5 μM G418 showed a significantly different amino acid insertion profile for two (UAG and UGA) of the three PTCs (*SI Appendix*, Table S1). With UAA as the PTC, the average of two independent experiments showed that the amino acid insertion pattern was similar to all other readthrough-inducing conditions with relatively comparable insertion frequencies of Gln (46.1%) and Tyr (51.8%) and a low insertion rate for Lys (1.9%) (Fig. 2*A*; *SI Appendix*, Table S1). With UGA as the PTC, insertion of the same amino acids (Trp, Arg, and Cys) was observed, but, compared with either endogenous readthrough events or ataluren treatment, significantly higher levels of Cys insertion (27.2%) were observed (Fig. 2*A*; *SI Appendix*, Table S1). Surprisingly, the amino acid insertion pattern at UAG was atypical after G418 treatment, with identification of 12 different amino acids at the PTC, some of which were inserted at very low levels (*SI Appendix*, Table S1). Lys was the predominant insertion at UAG with a frequency of 90% (*SI Appendix*, Table S1). Gln and Tyr, the other two amino acids that were normally inserted with

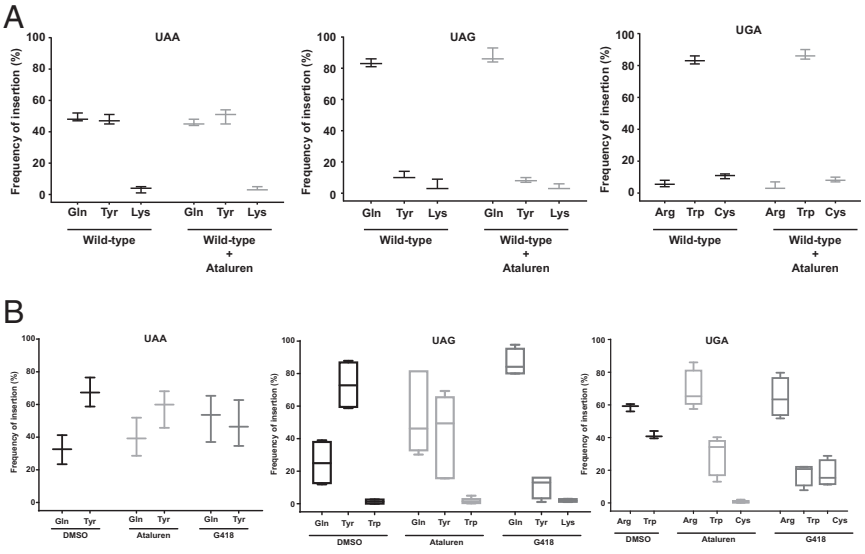

Fig. 2. Ataluren-mediated decoding of nonsense codons. Comparison of amino acid insertion at PTCs during termination readthrough of HA-*LUC*$_{(PTC20)}$-SF reporters after ataluren treatment in yeast and 293H cells. Epitope-tagged luciferase was purified from the respective cells and subjected to mass spectrometry analyses. Box and whisker graphs depict the amino acids inserted for each nonsense codon. Horizontal lines are the means and vertical lines are the SD. (*A*) Data from WT [*PSI*–] yeast cells treated with 30 μM ataluren (n = 3). (*B*) Data from 293H cells treated with 30 μM ataluren. Boxes represent the range of at least four determinations. Where there are no boxes, three determinations were done. Data used to generate graphs in *B* are in *SI Appendix*, Table S6.

much higher frequencies under all other conditions, were detected after G418 treatment, but with much lower frequencies of 4.7% and 1.5%, respectively (*SI Appendix*, Table S1). Treatment of cells with a higher concentration of G418 (15 μM) resulted in insertion of various amino acids at all three PTCs (*SI Appendix*, Table S2).

We next tested whether ataluren promoted insertion of similar sets of near-cognate tRNAs when HA-*LUC*$_{(PTC20)}$-SF alleles were expressed in human cells. As expected, 293H cells stably expressing HA-*LUC*$_{(PTC20)}$-SF alleles manifested increases in luciferase protein and activity after incubating the cells with ataluren or G418, and for all combinations other than UAA and ataluren these increases were clearly dependent upon the presence of a PTC in the luciferase allele (*SI Appendix*, Fig. S3 *C* and *D*). Luciferase readthrough products were purified and subjected to LC-MS/MS analyses as described above. Endogenous readthrough products purified from cells treated with 0.02% DMSO showed incorporation of two amino acids when UAA was the PTC: Gln (32.4 ± 8.9%) and Tyr (67.5 ± 8.9%) (Fig. 2*B*). When UAG was the PTC, Tyr (73.1 + 15%), Gln (25.2 ± 13.7%), and Trp (1.3 ± 1.4%) were inserted (Fig. 2*B*). Surprisingly, the decoding of UAG by Trp-tRNA is indicative of mispairing at the second position of the nonsense codon (*SI Appendix*, Table S3), a phenomenon not seen with yeast reporters or with the other two nonsense codons in these cells. Analysis of UGA endogenous readthrough products revealed insertion of Trp (41.4 ± 2.3%) and Arg (58.6 ± 2.3%) (Fig. 2*B*).

Characterization of readthrough products from 293H cells treated with ataluren (30 μM) showed insertion of Tyr (57.9 ± 11.3%) and Gln (39.9 ± 11.7%) at UAA; insertion of Tyr (43.9 ± 20.9%), Gln (53.2 ± 20.3%), and Trp (1.8 ± 1.9%) at UAG; and insertion of Arg (69.7 ± 11.3%), Trp (28.8 ± 11.4%), and Cys (0.7 ± 0.7%) at UGA (Fig. 2*B*). For UAA and UAG, the ataluren-induced readthrough products were similar to the endogenous readthrough products in identity and relative insertion frequencies for the respective amino acids. UGA readthrough products from ataluren-treated cells showed a low but consistent frequency of Cys insertion that was not observed in the endogenous readthrough products. Treatment of human cells with another small-molecule readthrough effector, G418 (150 μM), resulted in the insertion of Tyr (47.9 ± 14.1%) and Gln (52 ± 14.2%) at UAA; Gln (86.5 ± 8.3%), Tyr (10.8 ± 7.0%), and Lys (2.0 ± 0.8%) at UAG; and Arg (64.5 ± 11.8%), Trp (17.9+6.8%), and Cys (17.7 ± 8.0%) at UGA (Fig. 2*B*). Thus, G418 treatment yielded a pattern and frequency of amino acid insertion that differed significantly from endogenous readthrough, with the greatest difference at the UAG PTC, followed by UGA, and then UAA. Comparisons to endogenous readthrough indicated that G418 altered PTC decoding in both yeast and human cells and in part may reflect G418's interference with the decoding process (1, 27). This was found to be true for another aminoglycoside readthrough effector, gentamicin, in both yeast (21) and human cells (*SI Appendix*, Table S4).

Readthrough Products Are Functional. We used three approaches to determine whether the readthrough products synthesized after ataluren or aminoglycoside treatment result in functional proteins. First, the growth of yeast cells harboring the HA-*HIS3*$_{(UAA100)}$-SF allele was monitored when media lacking histidine was or was not supplemented with readthrough-promoting drugs. In *SI Appendix*, Fig. S8*A* shows that cell growth was restored after ataluren (or gentamicin) treatment, demonstrating that the amino acids inserted at the HA-*HIS3*$_{(UAA100)}$-SF PTC result in functional readthrough products. Second, we assessed the functionality of ataluren-induced luciferase readthrough products by replacing the WT glycine residue at position 20 with the six different amino acids identified in the yeast-based mass spectrometry analyses of Fig. 2*A*. These comparisons demonstrated comparable activity from all position 20 substitutions (*SI Appendix*, Fig. S8*B*), indicating that, at least with respect to luciferase position 20, enzymatic activity is unlikely to be affected by ataluren- or G418-mediated readthrough. Finally, we determined whether protein produced via readthrough therapy from a disease-causing nonsense allele could also retain function. Recognizing that G542X is the most frequent *CFTR* nonsense mutation (28), we used that allele to test this possibility. CFTR is a large, hydrophobic protein of generally low abundance, the expression of which is normally limited to epithelial cells. Because previous studies have shown that the local sequence context around a PTC acts as a primary determinant of readthrough efficiency (29, 30), we inserted the *CFTR-G542X* mutation (TGA) and its local sequence context (three codons on either side) into a construct amenable to protein purification from HEK293 cells and mass spectrometry. This construct contained TGFP, the *CFTR-G542X* mutation and context, and C-terminal HA and 6× His tags (*SI Appendix*, Fig. S1*D*). After PTC suppression, the full-length protein will contain TGFP, along with the HA and His tags, whereas the prematurely terminated protein will contain TGFP only. We observed an increase of full-length protein production after G418 (150 μM) treatment of HEK293 cells harboring this reporter (Fig. 3*A*) and then identified the amino acids inserted at the PTC of the *TGFP-CFTR-542X* mRNA with G418 treatment. Consistent with the data obtained from *LUC* reporters in yeast and 293H cells, the same three amino acids (Arg, Cys, and Trp) were identified in this UGA suppression reporter system, but with different frequencies (*SI Appendix*, Fig. S9 and Table S5).

We then determined if these amino acid substitutions affected CFTR function. Site-directed mutagenesis was used to change the

position 542 Gly codon to Arg, Cys, or Trp codons in a full-length cDNA. Transient transfections were then used to introduce each construct into HEK293 cells, and the core glycosylated (band B) and mature (band C) forms of CFTR were visualized by Western blotting (Fig. 3*B*). We found that the cell lines expressing the G542R and G542C forms of CFTR exhibited less maturation of band B to band C than WT CFTR, whereas the G542W cell line did not exhibit any band C. These results suggest that these three CFTR variants at position G542 either cause a partial defect in maturation of the endoplasmic reticulum (ER) form of CFTR to the mature cell-surface form or reduce the stability of the mature form of CFTR at the cell surface (Fig. 3*B*). To address these potential defects at the functional level, we constructed stable cell lines by transfecting the WT CFTR, CFTR-G542X, G542R, G542C, or G542W constructs into Fischer rat thyroid (FRT) cells, a cell type for which the conditions required for cell growth, PTC readthrough, and electrophysiological assays were compatible with G418 treatment. Using these stable FRT cell lines grown to confluence on filters, we performed short-circuit current (Isc) and transepithelial chloride conductance (Gt) assays to measure CFTR function. Forskolin was used to activate CFTR, and the CFTR inhibitor $CFTR_{Inh}$-172 was used to confirm the specificity of CFTR function. To correct for any differences in CFTR expression, these measurements were then normalized to the *CFTR* mRNA level measured in each stable cell line by qPCR analysis. As expected, all three G542 substitutions displayed lower CFTR activity than WT (Fig. 3 *C* and *D*). G542R and G542C showed ∼40–70% of WT Isc, which correlates well with less band C (Fig. 3*B*). We measured a corrected CFTR activity of only ∼10% for G542W, consistent with little or no band C observed in the Western blot. Taken together, these results demonstrate that CFTR variants resulting from readthrough retain variable but significant functionality.

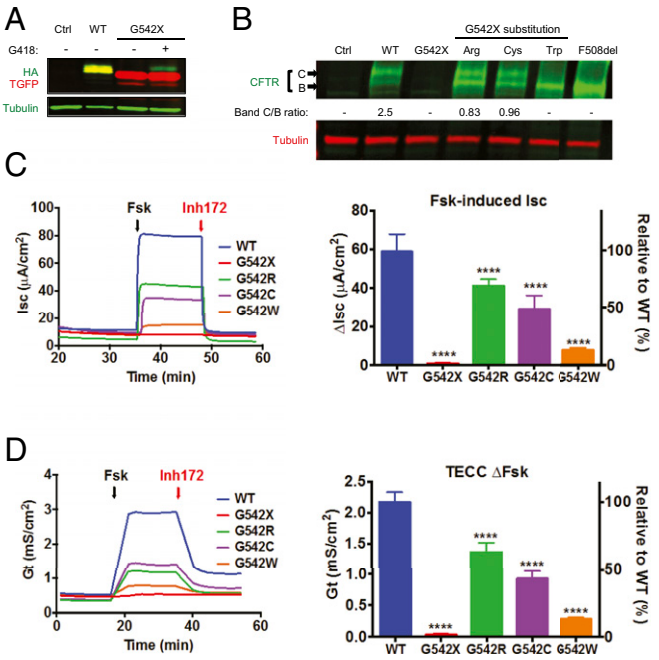

Fig. 3. Characterization of the amino acid insertions at human *CFTR-G542X*. (*A*) Western blot showing an increased amount of full-length protein (containing both TGFP and HA tag) (yellow-green bands) compared to the TGFP protein lacking the HA tag (red bands) after G418 treatment in HEK293 cells transiently transfected with the G542X construct. (*B*) Western blot showing the level of CFTR maturation observed in HEK293 cells transiently transfected with *CFTR* G542 variants. "Band B" is the ER form of CFTR, whereas "Band C" is the mature form. CFTR-F508del is a mutant form of CFTR that is retained in the ER and consequently only produces Band B. (*C*) Representative tracings (*Left*) and quantitation results (*Right*) of short-circuit current (Isc) measurements of CFTR chloride channel activity in FRT epithelial cell monolayers stably expressing the *CFTR* G542 variant constructs. (*D*) Representative tracings (*Left*) and quantitation (*Right*) of Conductance (Gt) measurements of CFTR chloride channel activity in FRT monolayers stably expressing the *CFTR* G542 variant constructs.

Rules of Near-Cognate tRNA Insertion. With the exception of some aspects of G418-mediated nonsense suppression treatment, which may be atypical (see above), a comparison of the amino acids inserted at PTCs under different readthrough-inducing conditions, as well as with different reporters, shows considerable similarity in yeast and mammalian cells. In both organisms, Gln, Lys, and Tyr are inserted at UAA and UAG, and Trp, Arg, and Cys are inserted at UGA (Fig. 2; *SI Appendix*, Tables S1, S2, S4, and S6) (21, 26). Our analyses of readthrough products indicate that such biases arise, in part, because some nonstandard codon:anticodon base pairs are preferred over others (*SI Appendix*, Table S3). For example, in all instances where individual tRNA choices can be identified, position 1 U-G mispairing appears to be preferred over U-U (Fig. 2; *SI Appendix*, Tables S1, S2, S4, and S6) (21). Furthermore, the lack of Gly insertion at UGA and Gln insertion at UAA or UAG (with the exception of G418 treatment) suggests that U-C mispairing at position 1 of the codon is not readily accommodated. Given that the decoding center of the ribosome is geometrically constrained (31, 32), the structure of the base pairs might be key determinants of mispairing. Alternatively, the relative abundance of tRNAs may govern insertion frequencies. To assess whether favored geometry of certain base pairs or tRNA abundance is the key parameter for this bias, we examined tRNA utilization in UGA readthrough. When UGA is the PTC, yeast cells show preferential insertion of Trp whereas 293H cells prefer insertion of Arg (Fig. 2 *A* and *B*). Arg insertion at UGA can be mediated by two near-cognate tRNAs: tRNA-Arg-UCG (using U-G mispairing at position 1 of the codon) and tRNA-Arg-UCU (using U-U mispairing at position 1 of the codon) (*SI Appendix*, Table S3). In yeast, Arg insertion at UGA most likely occurs by mispairing of tRNA-Arg-UCU, as tRNA-Arg-UCG expression has not been observed in these cells (33). On the other hand, tRNA-Arg-UCG is expressed in mammalian cells (33), and their insertion of Arg could be mediated via either of the Arg near-cognate tRNAs. We introduced and overexpressed a recombinant tRNA-Arg-UCG in WT [*PSI*−] yeast cells and monitored the insertion of Arg in the readthrough products. As a control, we overexpressed the endogenous tRNA-Arg-UCU. Northern analyses of total RNA isolated from the cells overexpressing the corresponding tRNA-Arg plasmids show considerable and comparable overexpression of the respective tRNA-Arg species (*SI Appendix*, Fig. S10*A*). A comparison of the luciferase activity from these strains showed that cells expressing tRNA-Arg-UCG also showed increased luciferase activity (*SI Appendix*, Fig. S10*B*), indicating that the expression of this specific tRNA correlated with enhanced readthrough efficiency. Moreover, expression of the recombinant tRNA-Arg-UCG shifted the bias toward Arg insertion at a frequency of 89.3 ± 1.5%, in contrast to a frequency of 6.6 ± 3% in WT cells (*SI Appendix*, Fig. S10*C*). In comparison, overexpression of the endogenous tRNA-Arg-UCU in yeast cells increased the frequency of Arg insertion to 30.6 ± 4.7% (*SI Appendix*, Fig. S10*C*). These observations are consistent with the notion that U-G codon:anticodon mispairing is favored over U-U mispairing in position 1.

We also tested whether a U-C codon:anticodon mispairing event can be introduced at position 1 by overexpressing the corresponding near-cognate tRNA, tRNA-Glu-UUC. Even though strains overexpressing tRNA-Glu-UUC showed increased levels of the tRNA species compared with WT (*SI Appendix*, Fig. S10*D*), the readthrough efficiency, as monitored by luciferase activity, was not altered (*SI Appendix*, Fig. S10*E*), and the readthrough products from those cells showed insertion of the same three amino acids; i.e., Glu insertion was still not observed (*SI Appendix*, Fig. S10*F*). Taken together, these data suggest that some nonstandard base pairs are favored over others for near-cognate tRNA insertion at PTCs and that the geometry of the base pairs is the most likely determinant of this bias.

The Ribosome as a Likely Target of Ataluren. In a recent clinical trial (12), cystic fibrosis patients with nonsense mutations failed to show a

significant response to ataluren if they were concurrently being treated with inhaled tobramycin, an aminoglycoside with strong affinity for the ribosomal A site (34). This observation suggested that tobramycin might be an inhibitor of ataluren's nonsense suppression activity, a possibility considered in the experiments of Fig. 4. In HEK293 cells, stably expressing the W12X NanoLuc reporter treatment with a wide range of tobramycin concentrations failed to elicit any detectable readthrough activity of the drug (Fig. 4). However, in cells manifesting substantial ataluren-mediated readthrough of the PTC-containing NanoLuc mRNA, addition of tobramycin showed strong, dose-dependent reduction of ataluren's readthrough activity (Fig. 4), consistent with previous work showing that aminoglycosides reduce the ability of ataluren to promote readthrough but non-aminoglycoside antibiotics have no effect (12). Quantitation of this effect indicated that tobramycin inhibition of ataluren's activity had an IC_{50} of 20 μM (Fig. 4). These results not only provide insight into the results of the aforementioned clinical trial, but also suggest that ataluren, like tobramycin, might also bind to the ribosome and thus affect near-cognate tRNA selection during readthrough.

Discussion

Therapeutic nonsense suppression is a potentially powerful approach to the treatment of the large number of genetic disorders caused by nonsense mutations, and several small-molecule drugs are being investigated for their capability to engender such therapy (1, 2). Multiple experimental approaches with cell lines, patient cells, animal models, and genetic disorder patients have demonstrated that the drug ataluren can restore expression to genes and mRNAs otherwise inactive because of the presence of premature nonsense codons (1, 3–14, 23). Collectively, such experiments have strongly suggested that ataluren promotes nonsense suppression, i.e., the insertion of near-cognate tRNAs at PTCs, but direct evidence for this activity has been lacking. Here, we determined the amino acid sequences of full-length *LUC* and chimeric *CFTR* proteins accumulating in control and readthrough effector-treated yeast and human cells, an approach that leads us to conclude that ataluren does indeed stimulate the incorporation of near-cognate tRNAs at PTCs. Notably, our analysis of the products of ataluren-induced PTC readthrough demonstrates that a distinct subset of amino acids is inserted during nonsense suppression of reporter and disease-related mRNAs in human cells. These results, the observation that the amino acid insertions occurring as a consequence of ataluren treatment are similar but not identical to those occurring endogenously (Fig. 2), and the finding that tobramycin specifically antagonizes the restoration of NanoLuc activity from a PTC allele by ataluren (Fig. 4) negate other hypotheses that sought to explain ataluren's mechanism of action (17, 18).

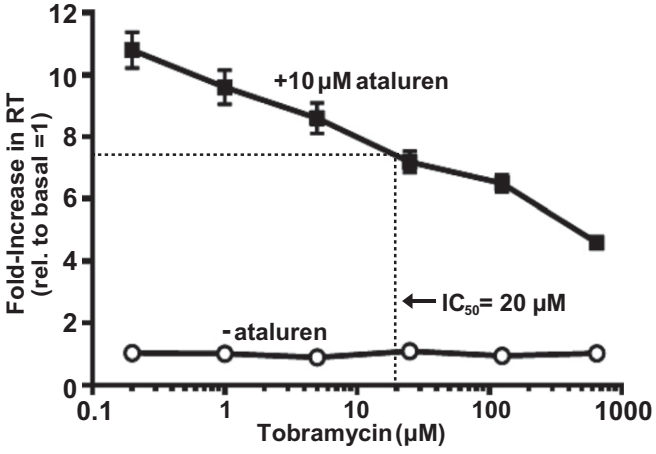

Fig. 4. Tobramycin is a potent inhibitor of ataluren-mediated readthrough. The effect of tobramycin on NanoLuc activity in HEK293 cells expressing a UGA (W12X) NanoLuc reporter with either no prior treatment or following treatment with 10 μM ataluren for 48 hours. Initial stimulation of readthrough by ataluren in the absence of tobramycin was 15-fold above background.

Ataluren's enhancement of near-cognate tRNA insertion favors a subset of tRNAs, generally leading to incorporation of Gln, Lys, and Tyr at UAA and UAG codons and of Trp, Arg, and Cys at UGA codons. The weak readthrough activity seen here with the HA-$LUC_{(UAA20)}$-SF allele is atypical of that seen with UAA PTCs in other mRNAs (3, 4, 14) and most likely reflects the influence of codon context on readthrough (29). Ataluren's influence over the extent of specific tRNA selection implies that this drug's target could be the ribosome, a conclusion consistent with the drug's markedly diminished efficacy in the presence of tobramycin (Fig. 4), an aminoglycoside known to bind to the ribosome's A site (34). The apparent tRNA selection bias also suggests that both endogenous and ataluren-stimulated near-cognate tRNA mispairing are not random processes and that factors contributing to the apparent preferences are conserved. One component of this selection process is a set of favored mispairings, primarily at codon position 1, where U-G mispairing is preferred over U-U and where U-C mispairing is strongly disfavored (Fig. 2; *SI Appendix*, Table S3) (21). As noted previously (21), U-G mispairing at position 1 is likely to be favored because of its ability to act as a geometric mimic of a U-A base pair (32). It is also plausible that the stability of nonstandard base pairs in position 1 is enhanced by modification of neighboring tRNA anticodon bases, e.g., thiolation of the wobble position uridine (35). At position 3, multiple nonstandard mispairings are tolerated including A-C, G-G, A-G, and possibly others (Fig. 2; *SI Appendix*, Table S3) (21). Another determinant of tRNA insertion choice is the extent to which the tRNA is expressed, if at all. As shown in the experiments in *SI Appendix*, Fig. S10*C*, yeast cells prefer Trp insertion over Arg insertion at UGA, largely because they lack tRNA-Arg-UCG, a tRNA that allows U-G mispairing. When tRNA-Arg-UCG was provided, it both stimulated readthrough and led to a marked increase in the relative frequency of Arg insertion at the PTC, unlike tRNA-Arg-UCU overexpression (*SI Appendix*, Fig. S10*C*) (36).

An important observation from these experiments is that the readthrough products of ataluren- or aminoglycoside-mediated nonsense suppression tested here are at least partially functional and, in many cases, fully functional. Earlier experiments with reporter genes, cultured cells, mouse models, and clinical trials of human DMD and CF nonsense mutation patients indicated that readthrough products are functional (1, 3–13, 23, 37–39), but could not address the question of specific amino acid substitutions at specific codon positions. Although our studies have addressed substitutions in only a limited number of positions in luciferase, His3, and CFTR, it is nevertheless reassuring with respect to the potential of therapeutic nonsense suppression that all of the substitutions analyzed here retained some degree of function. It will be of interest to determine whether the observed activities can be increased by parallel approaches, e.g., antagonists of mRNA decay (2), specific protein correctors or potentiators [as have been successfully used for CFTR (39)], or enhancers of the expression of certain tRNAs.

The efficacy of therapeutic nonsense suppression will also depend on the relative toxicity of the drug used to promote specific PTC readthrough. Ataluren has been shown to exhibit a favorable safety profile (27), and we speculate that at least two aspects of its activity support this attribute. First, as discussed above, ataluren stimulates PTC insertion of a set of near-cognate tRNAs that closely resemble those inserted endogenously at much lower levels. As a consequence, the full-length proteins that accumulate in ataluren-treated cells are unlikely to have antigenic differences from the repertoire of readthrough proteins normally accumulating in a patient, albeit at low levels. This low-level expression of full-length proteins by endogenous readthrough of nonsense-containing mRNAs may be sufficient to allow the polypeptides that accumulate during ataluren-stimulated readthrough to be recognized as "self" by the immune system, thus minimizing the potential for an autoimmune reaction. Second, at least compared with G418, ataluren generally has modest readthrough activity, showing only readthrough of premature termination events, but lacking readthrough

activity on the considerably more efficient process of normal termination (3, 40). Ataluren's failure to promote detectable readthrough of normal termination codons undoubtedly minimizes the possible accumulation of C-terminally extended proteins and their likely inhibitory activity and immunogenicity. In this regard, the much higher readthrough activity of G418, as well as its deviation from the pattern of endogenous insertion of near-cognate tRNAs, may contribute to that drug's known toxicity (2). These results increase our understanding of readthrough therapies and how they might be tailored to specific disease alleles.

Materials and Methods

Detailed methods, given in *SI Appendix, SI Materials and Methods*, are summarized here.

Reporter and Expression Plasmids. *LUC*- and *HIS3*-based reporters were used to analyze readthrough in yeast, and NanoLuc-, H2B-GFP-, p53-, *LUC*-, and TGFP-based reporters were used for the same purpose in human cells. For yeast, the construction and use of epitope-tagged *LUC*-PTC$_{20}$ reporters has been described previously (21); the *HIS3*-PTC$_{100}$ reporter used comparable epitope tags. In human cells, (*i*) using oligonucleotides DB4084 and DB4085 (*SI Appendix*, Table S7), UGA was introduced at codon 12 of the NanoLuc ORF expressed from pFN[Nluc/CMV/Neo] (Promega); (*ii*) the H2B-GFP reporter was constructed as described by Lentini et al. (6); (*iii*) UGA PTCs at positions 196 or 213 of the p53 ORF were introduced using site-directed mutagenesis, and the respective constructs were expressed from pcDNA 3.1 Hygro(+); (*iv*) *LUC*-$_{PTC20}$ constructs used in yeast were modified to include *TPI1* intron 6 at nucleotide 239 and expressed from pSELECT Zeo; (*v*) *CFTR-G542X* (UGA) and *CFTR-WT*, along with codons 539–541 and 543–545, were fused to TurboGFP (TGFP) along with HA and 6× His tags and expressed from pcDNA 3.1 Zeo(+); and (*vi*) *CFTR*-G542R, G542C, and G542W were created by site-directed mutagenesis of a WT *CFTR* cDNA and expressed from pcDNA 3.1 Zeo(+).

RNA and Protein Analyses. Procedures for RNA analysis, protein purification, and luciferase assays were as described previously (3, 19, 21, 38) or in *SI Appendix*. Western analyses and protein purification largely used antibodies or affinity resins targeted to the HA, FLAG, StrepII, T-GFP, and 6× His epitope tags expressed from the respective reporter constructs.

Amino Acid Sequence Analysis of Luciferase and GFP-CFTR Readthrough Products. Luciferase readthrough proteins were purified by epitope tag affinity chromatography and gel electrophoresis, subjected to proteolytic digestion, and analyzed by LC-MS/MS as described previously (21) and in *SI Appendix*. Raw data files were subjected to database searches, using SwissProt indices for *Saccharomyces cerevisiae* and human polypeptides. Comparable analyses based on CFTR used SEQUEST searches and Scaffold Q+.

ACKNOWLEDGMENTS. We are indebted to Elizabeth Grayhack and Christina Brule for generously providing tRNA expression plasmids and Shirley Yeh and Angela Esteves for technical support. This work was supported by National Institutes of Health Grants R37 GM27757 (to A.J.), R21 NS090928 (to D.M.B.), R21NS090928 (to K.M.K.), and P30 DK072482 (to S.M.R.); by the Cystic Fibrosis Foundation (D.M.B. and S.M.R.); and by the University of Alabama Institutional Core Support Program from National Cancer Institute Grant P30CA13148-38 (to J.M.)

1. Peltz SW, Morsy M, Welch EM, Jacobson A (2013) Ataluren as an agent for therapeutic nonsense suppression. *Annu Rev Med* 64:407–425.
2. Keeling KM, Xue X, Gunn G, Bedwell DM (2014) Therapeutics based on stop codon readthrough. *Annu Rev Genomics Hum Genet* 15:371–394.
3. Welch EM, et al. (2007) PTC124 targets genetic disorders caused by nonsense mutations. *Nature* 447(7140):87–91.
4. Li M, Andersson-Lendahl M, Sejersen T, Arner A (2014) Muscle dysfunction and structural defects of dystrophin-null sapje mutant zebrafish larvae are rescued by ataluren treatment. *FASEB J* 28(4):1593–1599.
5. Gregory-Evans CY, et al. (2014) Postnatal manipulation of Pax6 dosage reverses congenital tissue malformation defects. *J Clin Invest* 124(1):111–116.
6. Lentini L, et al. (2014) Toward a rationale for the PTC124 (Ataluren) promoted readthrough of premature stop codons: A computational approach and GFP-reporter cell-based assay. *Mol Pharm* 11(3):653–664.
7. Drake KM, Dunmore BJ, McNelly LN, Morrell NW, Aldred MA (2013) Correction of nonsense BMPR2 and SMAD9 mutations by ataluren in pulmonary arterial hypertension. *Am J Respir Cell Mol Biol* 49(3):403–409.
8. Goldmann T, Overlack N, Wolfrum U, Nagel-Wolfrum K (2011) PTC124-mediated translational readthrough of a nonsense mutation causing Usher syndrome type 1C. *Hum Gene Ther* 22(5):537–547.
9. Sánchez-Alcudia R, Pérez B, Ugarte M, Desviat LR (2012) Feasibility of nonsense mutation readthrough as a novel therapeutical approach in propionic acidemia. *Hum Mutat* 33(6):973–980.
10. Haas M, et al. (2015) European Medicines Agency review of ataluren for the treatment of ambulant patients aged 5 years and older with Duchenne muscular dystrophy resulting from a nonsense mutation in the dystrophin gene. *Neuromuscul Disord* 25(1):5–13.
11. Bushby K, et al.; PTC124-GD-007-DMD STUDY GROUP (2014) Ataluren treatment of patients with nonsense mutation dystrophinopathy. *Muscle Nerve* 50(4):477–487.
12. Kerem E, et al.; Cystic Fibrosis Ataluren Study Group (2014) Ataluren for the treatment of nonsense-mutation cystic fibrosis: A randomised, double-blind, placebo-controlled phase 3 trial. *Lancet Respir Med* 2(7):539–547.
13. Finkel RS, et al. (2013) Phase 2a study of ataluren-mediated dystrophin production in patients with nonsense mutation Duchenne muscular dystrophy. *PLoS One* 8(12):e81302.
14. Moosajee M, et al. (June 21, 2016) Functional rescue of REP1 following treatment with PTC124 and novel derivative PTC-414 in human choroideremia fibroblasts and the nonsense-mediated zebrafish model. *Hum Mol Genet*, pii: ddw184.
15. Sermet-Gaudelus I, et al. (2010) Ataluren (PTC124) induces cystic fibrosis transmembrane conductance regulator protein expression and activity in children with nonsense mutation cystic fibrosis. *Am J Respir Crit Care Med* 182(10):1262–1272.
16. Kerem E, et al. (2008) Effectiveness of PTC124 treatment of cystic fibrosis caused by nonsense mutations: A prospective phase II trial. *Lancet* 372(9640):719–727.
17. McElroy SP, et al. (2013) A lack of premature termination codon read-through efficacy of PTC124 (Ataluren) in a diverse array of reporter assays. *PLoS Biol* 11(6):e1001593.
18. Auld DS, Thorne N, Maguire WF, Inglese J (2009) Mechanism of PTC124 activity in cell-based luciferase assays of nonsense codon suppression. *Proc Natl Acad Sci USA* 106(9):3585–3590.
19. Hall MP, et al. (2012) Engineered luciferase reporter from a deep sea shrimp utilizing a novel imidazopyrazinone substrate. *ACS Chem Biol* 7(11):1848–1857.
20. Kuroha K, Tatematsu T, Inada T (2009) Upf1 stimulates degradation of the product derived from aberrant messenger RNA containing a specific nonsense mutation by the proteasome. *EMBO Rep* 10(11):1265–1271.
21. Roy B, Leszyk JD, Mangus DA, Jacobson A (2015) Nonsense suppression by near-cognate tRNAs employs alternative base pairing at codon positions 1 and 3. *Proc Natl Acad Sci USA* 112(10):3038–3043.
22. Auld DS, et al. (2010) Molecular basis for the high-affinity binding and stabilization of firefly luciferase by PTC124. *Proc Natl Acad Sci USA* 107(11):4878–4883.
23. Zhou Y, Jiang Q, Takahagi S, Shao C, Uitto J (2013) Premature termination codon read-through in the ABCC6 gene: Potential treatment for pseudoxanthoma elasticum. *J Invest Dermatol* 133(12):2672–2677.
24. Green L, Goff SP (2015) Translational readthrough-promoting drugs enhance pseudoknot-mediated suppression of the stop codon at the Moloney murine leukemia virus gag–pol junction. *J Gen Virol* 96(11):3411–3421.
25. Peltz SW, et al. (2009) Nonsense suppression activity of PTC124 (ataluren). *Proc Natl Acad Sci USA* 106(25):E64; author reply E65.
26. Blanchet S, Cornu D, Argentini M, Namy O (2014) New insights into the incorporation of natural suppressor tRNAs at stop codons in Saccharomyces cerevisiae. *Nucleic Acids Res* 42(15):10061–10072.
27. Hirawat S, et al. (2007) Safety, tolerability, and pharmacokinetics of PTC124, a nonaminoglycoside nonsense mutation suppressor, following single- and multiple-dose administration to healthy male and female adult volunteers. *J Clin Pharmacol* 47(4):430–444.
28. Bobadilla JL, Macek M, Jr, Fine JP, Farrell PM (2002) Cystic fibrosis: A worldwide analysis of CFTR mutations: Correlation with incidence data and application to screening. *Hum Mutat* 19(6):575–606.
29. Manuvakhova M, Keeling K, Bedwell DM (2000) Aminoglycoside antibiotics mediate context-dependent suppression of termination codons in a mammalian translation system. *RNA* 6(7):1044–1055.
30. Keeling KM, Bedwell DM (2002) Clinically relevant aminoglycosides can suppress disease-associated premature stop mutations in the IDUA and P53 cDNAs in a mammalian translation system. *J Mol Med (Berl)* 80(6):367–376.
31. Westhof E, Yusupov M, Yusupova G (2014) Recognition of Watson-Crick base pairs: Constraints and limits due to geometric selection and tautomerism. *F1000Prime Rep* 6:19.
32. Demeshkina N, Jenner L, Westhof E, Yusupov M, Yusupova G (2013) New structural insights into the decoding mechanism: Translation infidelity via a G·U pair with Watson-Crick geometry. *FEBS Lett* 587(13):1848–1857.
33. Tuller T, et al. (2010) An evolutionarily conserved mechanism for controlling the efficiency of protein translation. *Cell* 141(2):344–354.
34. Salian S, et al. (2012) Structure-activity relationships among the kanamycin aminoglycosides: Role of ring I hydroxyl and amino groups. *Antimicrob Agents Chemother* 56(12):6104–6108.
35. Kumar RK, Davis DR (1997) Synthesis and studies on the effect of 2-thiouridine and 4-thiouridine on sugar conformation and RNA duplex stability. *Nucleic Acids Res* 25(6):1272–1280.
36. Beznosková P, Gunišová S, Valášek LS (2016) Rules of UGA-N decoding by near-cognate tRNAs and analysis of readthrough on short uORFs in yeast. *RNA* 22(3):456–466.
37. Bedwell DM, et al. (1997) Suppression of a CFTR premature stop mutation in a bronchial epithelial cell line. *Nat Med* 3(11):1280–1284.
38. Du M, et al. (2008) PTC124 is an orally bioavailable compound that promotes suppression of the human CFTR-G542X nonsense allele in a CF mouse model. *Proc Natl Acad Sci USA* 105(6):2064–2069.
39. Xue X, et al. (2014) Synthetic aminoglycosides efficiently suppress cystic fibrosis transmembrane conductance regulator nonsense mutations and are enhanced by ivacaftor. *Am J Respir Cell Mol Biol* 50(4):805–816.
40. Amrani N, et al. (2004) A *faux* 3′-UTR promotes aberrant termination and triggers nonsense-mediated mRNA decay. *Nature* 432(7013):112–118.

Supporting Information

SI Materials and Methods

Readthrough Drugs

PTC Therapeutics, Inc. supplied ataluren for this study. Ataluren was dissolved in dimethylsulfoxide (DMSO) and cultured cells were treated such that the final DMSO concentration was 0.3% (vol/vol). Tobramycin, geneticin (G418), and gentamicin were purchased from Sigma and were administered in PBS.

Plasmid Construction

a) Yeast expression plasmids

i. *LUC* reporters. Construction and use of epitope-tagged *LUC*-based PTC_{20} reporters has been described previously (1).

ii. *HIS3* reporter. The wild-type HA-*HIS3*-SF and the PTC-containing HA-*HIS3*$_{(UAA100)}$-SF constructs consist of the yeast *TPI1* promoter followed by an N-terminal 3X Hemaglutinin (HA) tag fused in-frame with the *HIS3* gene (with/without an in-frame stop codon at *HIS3* position 100), followed by in-frame StrepII and FLAG tags and the *TPI1* 3' UTR. The plasmids harboring either the wild-type or the PTC-containing *HIS3* cassette were generated by PCR and standard molecular cloning techniques, and fragments were inserted into yEplac181 after digestion of the respective restriction sites.

b) Mammalian expression plasmids

i. NanoLuc reporters. The pFN[Nluc/CMV/Neo] plasmid containing the NanoLuc open reading frame was purchased from Promega Corporation (CS181701). Using site-directed mutagenesis and oligonucleotides DB4084 and DB4085 (Supp. Table 7), a point mutation was introduced into NanoLuc at codon 12, which changed the tryptophan codon (UGG) to a UGA PTC. Using standard techniques, the WT and W12X NanoLuc open reading frames were then subcloned into the NheI and XhoI sites of pcDNA3.1Zeo(-) (Invitrogen). These plasmid constructs were subsequently transfected into 293H cells and stable transfectants were selected using 0.2 mg/ml zeocin (Invitrogen) for three weeks.

ii. p53 reporters. Alleles of the p53 ORF were synthesized with TGA nonsense mutations at positions 196 or 213 and then cloned into pcDNA3.1/Hygro(+) using standard techniques. The plasmids were then transfected into either CALU-6 or HDQ cell lines.

iii. H2B-GFP reporter. This reporter encompasses a histone H2B coding sequence fused to that of GFP, with the TGG codon at nucleotide positions 172-174 of the GFP ORF mutated to TGA. Construction of the vector was as described by Lentini *et al*. (2)

iv. *LUC* reporters. The luciferase reporter system used for readthrough analyses in mammalian cells is similar to the set of yeast luciferase readthrough reporters used in Roy *et al.* (1), with a few modifications. Intron 6 from the yeast *TPI1* gene was introduced into the *LUC* coding sequence at nucleotide 239, downstream of the PTC_{20} insertion site. The HA-*LUC*2-SF cassette (wild-type or PTC-containing) was then cloned into corresponding restriction sites in the pSELECT Zeo MCS using standard molecular biology techniques.

v. TGFP reporter. *CFTR-G542X* (UGA) or the corresponding wild-type along with the G542X context (three codons upstream and downstream) was fused to TurboGFP (TGFP) along with HA and 6XHis tags. This fragment was inserted into the pcDNA 3.1 Zeo(+) expression vector (Invitrogen). CFTR-G542R, G542C, and G542W were obtained through site-directed mutagenesis of a wild-type CFTR cDNA. The mutated fragment of CFTR was inserted into the CFTR cDNA in pcDNA 3.1 Zeo(+) and sequences were confirmed.

Yeast Cell Methods

a) Protein purification and analyses. Cells expressing HA-*LUC*-SF or HA-$LUC_{(PTC20)}$-SF were grown in synthetic complete (SC) medium lacking leucine with or without any drug treatment for readthrough induction. Readthrough products were purified as described previously (1). Briefly, cells were collected by rapid filtration and resuspended in Buffer W (100 mM Tris pH 8.0, 150 mM NaCl, 1 mM EDTA; supplemented with 0.1 mM DTT, 1 mM PMSF, and 1X protease inhibitor cocktail (Roche)). Cells were lysed using a cryoMill (Retsch) at 10 hertz for 20 min with constant liquid nitrogen cooling. Cell lysates

were clarified and luciferase was purified using Strep-Tactin resin according to the manufacturer's protocol (IBA, Germany). The efficiency of luciferase purification was monitored by analyzing fractions for luciferase activity, as well as by western blot analyses using anti-FLAG antibody (Sigma). Elution fractions from Strep-Tactin purification were concentrated using Amicon Ultra-15 30K NMWL filters (EMD Millipore) followed by analysis on 8% SDS-PAGE to resolve the readthrough product. Gels were silver stained (Proteosilver, Sigma) and processed for MS analysis. Three independent experiments were performed for all (one codon under one readthrough-inducing condition) except G418 treatment for which only two independent experiments were performed.

b) RNA analyses. Total RNA isolation and northern analyses were performed as described previously (1). Cells expressing either HA-*LUC*-SF or HA-*LUC*$_{(PTC20)}$-SF were grown in synthetic complete (SC) media lacking leucine. Random-primed DNA probes made from the 1.6 Kb NcoI-XhoI luciferase fragment or 129 bp XhoI-XbaI Strep-FLAG fragment were used to detect *LUC* mRNA and *HIS3* mRNA, respectively. Random-primed DNA probes made from the 0.6 Kb EcoRI-HindIII *CYH2* fragment, or the 0.5 Kb EcoRI *SCR1* fragment were used to detect the *CYH2* pre-mRNA, *CYH2* mRNA, and the *SCR1* RNA as controls for NMD and normalization, respectively. Transcript-specific signals were determined with a FUJI BAS-2500 analyzer.

For tRNA expression analysis, total tRNA was isolated from wild-type cells and cells overexpressing either tRNA-Arg-UCG (DL869) (3), tRNA-Arg-UCU (ECB1451), or tRNA-Glu-UUC (ELH239) as described previously (4). Isolated tRNAs (10 µg per sample) were resolved on a 6.5% polyacrylamide-8 M urea-0.1 M NaAc (pH 5.0) gel and electroblotted to Zeta-Probe membranes (Bio-Rad). ^{32}P-labeled oligonucleotides complementary to the tRNA of interest were used as probes. tRNA-specific signals were determined with a FUJI BAS-2500 analyzer.

c) Western analyses. Yeast cells (0.4 OD_{600} units per sample) were collected and processed as described previously (1). Samples were resolved by SDS-PAGE, transferred to Immobilon-P (Millipore) membranes, and incubated with anti-HA antibody (Sigma), anti-FLAG antibody (Sigma), or a monoclonal anti-Pgk1 antibody (Molecular Probes).

d) Protein half-life measurements. Readthrough product half-life was quantified as described previously (5). Yeast cells expressing HA-*HIS3*-SF or HA-*HIS3*$_{(PTC100)}$-SF reporters were treated with ataluren and were grown in synthetic complete (SC) media lacking leucine to log phase. Cycloheximide (50 µg/mL) was added to terminate protein synthesis followed by collection of equal number of cells at various time points and subjected to western blot analyses.

Mammalian Cell Methods

a) Protein purification and activity assays

i. NanoLuc activity assay. Prior to performing NanoLuc assays, zeocin was omitted from the media of the stable NanoLuc 293H cell lines for two passages due to its inhibitory effect on cell growth. WT and W12X reporter cells were then seeded into 96-well culture plates at a density of 4 x10^4 per well. When cells became ~50% confluent, they were treated with drugs for a period of 48 hours prior to assay. NanoLuc activity was measured using the Nano-Glo Luciferase Assay (Promega, N1110). All cells expressing the NanoLuc constructs were lysed in 50µl of 1X Passive Lysis Buffer (PLB) (Promega, E1941). However, the lysate of WT NanoLuc expressing cells was subsequently diluted 1:1000 with 1X passive lysis buffer. In a separate 96-well plate (Fisher 12-566-04), 5µl of the Nano-Glo Reagent were mixed with 5µl of each cell lysate and then incubated for 10 min at room temperature. Luciferase activity readings were then measured using a GloMax Multi Detection System (Promega). The data are expressed as the NanoLuc activity generated normalized to micrograms of total protein.

ii. Purification and analysis of *LUC* readthrough products. Wild-type or PTC-containing *LUC* expression plasmids were transfected into 293H cells (ThermoFisher Scientific) with FuGene 6 (Promega) and stable clones were selected using 300µg/mL Zeocin (ThermoFisher Scientific). Cells were harvested 72 hours after 30 µM ataluren treatment and 24 hours after 150 µM G418 (geneticin) treatment. Tandem purification of the readthrough products utilized C-terminal Strep or FLAG tags, followed by selection for the N-terminal HA tag. Briefly, cells were harvested in lysis buffer (FLAG purification: 0.025 M Tris, pH 7.4, 0.15 M NaCl, 0.001 M EDTA, 1% NP40, 5% glycerol; StrepTactin purification:100 mM Tris, pH 8.0, 150 mM NaCl, 1 mM EDTA) and the clarified lysates

were bound to either StrepTactin (Qiagen) or FLAG (Sigma) magnetic beads at 4ºC overnight according to the manufacturer's protocol. The eluates from the first purification were then bound to anti-HA magnetic beads for one hour and eluted by boiling the beads in 1X Laemmli Buffer (BioRad) for 10 min. The elution profile was monitored by measuring luciferase activity at each step in the purification process, using Bright-Glo (Promega) as a substrate and measured using a Perkin Elmer EnVision plate reader. The purified readthrough products were then analyzed on 10% SDS-PAGE, and gels were then silver stained (ProteoSilver, Sigma) and processed for mass spectrometry. At least three independent experiments were performed for each condition (each codon under one specific readthrough-inducing condition).

iii. Purification of GFP-CFTR readthrough products. 293H cells were harvested and lysed using three freeze and thaw cycles and a lysis buffer (pH 8.0, 50 mM NaH_2PO_4, 300 mM NaCl, 10 mM imidazole) containing a protease inhibitor cocktail tablet (Roche). The lysate was centrifuged and the supernatant was transferred to a new tube and incubated with Ni-NTA Superflow resin (Qiagen) overnight at 4ºC. The next day, the resin was washed three times with lysis buffer and eluted with elution buffer (pH 8.0, 50 mM NaH_2PO_4, 300 mM NaCl, 500 mM imidazole) four times.

b) Western analyses

i. Luciferase polypeptides. For detection of the readthrough products, 293H whole-cell lysates were electrophoresed through 10% (w/v) Bis-Tris polyacrylamide gels (ThermoFisher Technologies), transferred to a nitrocellulose membrane (BioRad), and incubated with anti-HA (1:1,000; ThermoFisher Technologies), anti-FLAG (1:1,000; Sigma), or anti- Firefly Luciferase (1:2,000; Rockland) antibodies. An anti-GAPDH antibody (1:10,000; Abcam) was used for normalization.

ii. GFP polypeptides. For the TGFP readthrough reporters, 293H cells were washed with 1X PBS, harvested, and lysed with lysis buffer. The lysate was centrifuged, boiled, and fractionated by electrophoresis on SDS-PAGE gels. Gels were transferred to Immobilon-FL PVDF membranes (EMD Millipore), which were then blocked using 5% (w/v) milk in PBST (0.3% Tween 20, v/v), incubated with anti-HA (Covance Research), anti-Tubulin (Abcam or DHSB), and anti-TGFP (Pierce) antibodies, followed by incubation with secondary antibodies IRDye 680RD and IRDye 800CW (Li-Cor) before imaging

using a Li-Cor Odyssey® CLx Infrared Imaging System. For CFTR western blots, cells were lysed with RIPA buffer containing a protease inhibitor tablet (Roche). The lysate was collected, incubated at 37°C for 30 min before electrophoresis, and then transferred and blotted as was done for TGFP proteins. CFTR antibodies were a 1:1 mixture of #570 and #596 monoclonal anti-CFTR antibodies from the University of North Carolina (http://www.unc.edu/~tjjensen/CFADP/index.html).

For the H2B-GFP readthrough products, 293H cell lysates were electrophoresed through 10% (w/v) Bis-Tris polyacrylamide gels (ThermoFisher Technologies), transferred to a nitrocellulose membrane (BioRad), and incubated with anti-GFP (1:1,000; Life Science Technologies) antibodies. An anti-GAPDH antibody (1:10,000; Abcam) was used for normalization.

iii. p53 polypeptides. The p53 readthrough products from cell lines expressing p53 nonsense alleles were detected using p53 MSD/ELISA (Meso Scale Discovery) using DO1 SC-126X (SantaCruz) and ab59243 (Abcam).

c) RNA analyses

i. *LUC* transcripts. Total RNA was extracted using RNeasy Mini Kit (Qiagen) as per the manufacturer's instructions. cDNA was synthesized using SuperScript III reverse transcriptase (Invitrogen). RNA samples were analyzed by Taqman-based RT-qPCR using luciferase specific primers (Table S7).

ii. GFP transcripts. Total RNA was extracted using RNeasy Mini Kit (Qiagen) as per the manufacturer's directions. cDNA was obtained through reverse transcription using iScript™ Reverse Transcription Supermix (Biorad). Quantitative real-time PCR was performed using the CFX96 Real-Time PCR Detection System (Biorad). Primer efficiencies for human CFTR discovered in Primerbank (http://pga.mgh.harvard.edu/primerbank/index.html) (5'-CCTATGACCC GGATAACAAG GA-3' and 5'-GAACACGGCT TGACAGCTTT A-3') and rat tubulin15 (5'-CAACACCTTC TTCAGTGAGA CAGG-3' and 5'-TCAATGATCT CCTTGCCAAT GGT-3') were 93.4% and 95.8%, respectively.

d) Functional assays in FRT monolayers

CFTR constructs were transfected into Fischer Rat Thyroid (FRT) cells and cell lines that stably express each CFTR cDNA were selected. Cells were seeded on Costar

24 well 0.4 µM permeable supports (Corning). After four days, confluent monolayers with tight junctions had formed, as measured by transepithelial resistance using an epithelial volt-ohm meter (WPI). Isc was measured in Ussing Chambers (Physiologic Instruments) using an 8-channel voltage clamp, while Gt was measured using a 24-channel voltage clamp (6).

Sample Preparation for Mass Spectrometry Analyses

a) Analyses of luciferase readthrough products. Full-length luciferase readthrough products resolved on SDS-polyacrylamide gels were excised after silver staining and the destained gel slices were subjected to endoproteinase Lys-C (Roche Diagnostics) digestion followed by LC-MS/MS analyses as described previously (1). Raw data files were subjected to database searching with Mascot Server (version 2.5) against the SwissProt index of *S. cerevisiae* (for yeast samples) and Human **(**for mammalian samples) that contain the sequences of all 20 potential codon 20 mutations of the *LUC* gene. The relative abundance of each amino acid at position 20 of luciferase was calculated by adding the corresponding precursor intensity of individual endo Lys-C peptides containing a codon 20 amino acid to yield a total peptide abundance that was then used to calculate the percentage of insertion of each amino acid (1).

b) Analyses of GFP-CFTR readthrough products. Full-length TGFP was purified using Ni-NTA Superflow resin (Qiagen). Protein fractions were resolved on an SDS Bis-Tris gel (Invitrogen) and gel bands corresponding to the molecular weight of interest were reduced, carbidomethylated, dehydrated, and digested with Trypsin Gold (Promega). Peptides were extracted, concentrated under vacuum, and resolubilized in 0.1% formic acid prior to analysis by 1D reverse phase LC-ESI-MS2 (7). Peptide digests were injected onto a Surveyor HPLC plus (Thermo Scientific) using a split flow configuration on the back end of a Jupiter C-18 column (Phenomenex). This system runs in-line with a Thermo Orbitrap Velos Pro hybrid mass spectrometer, equipped with a nano-electrospray source (Thermo Scientific), and all data were collected in CID mode. Data were searched using SEQUEST with a precursor mass window of 20ppm, trypsin digestion, variable modification C at 57.0293, and M at 15.9949. Searches were performed with a human subset of the UniRef100 database, which included common contaminants such as

digestion enzymes and human keratin, in addition to sequences specific to these experiments. A list of peptide IDs was generated based on SEQUEST search results, and which was then filtered using Scaffold Q+ (Protein Sciences). The filter cut-off values were set with peptide length (>5 AA's), no peptides with a MH+1 charge state were included, peptide probabilities were calculated and set to >90% C.I., with the number of peptides per protein set at two or more, and protein probabilities set to >99% C.I. Relative quantification across experiments was performed via spectral counting, and spectral count abundances were then normalized between samples. All spectra covering the sequences of interest were manually interpreted as a final quality control.

PTC124-AMP

a) Synthesis of PTC124-AMP. The compound was prepared as described by Auld *et al*. (8) (see their SI methods, compound 6). Briefly, a mixture of 3-(5-(2-fluorophenyl)-1,2,4-oxadiazol-3-yl)benzoic acid (0.2 g (0.70 mM) and ethyl-(N',N'-dimethylamino) propylcarbodiimide (EDC) 0.67 g (3.52 mM) in anhydrous DMF (4 mL) was stirred at room temperature for 10 min. Then adenosine-5-monophophate disodium salt 0.275 g (0.70 mM) and 4-dimethylamino-pyridine (DMAP) 9 mg (0.07 mM) were added and stirred vigorously at room temperature for one hour. The crude product was purified by preparative HPLC and lyophilized to get the free acid as a white powder. The free acid was then dissolved in 0.1 M ammonium bicarbonate solution and lyophilized to obtain the ammonium salt of the PTC124-AMP adduct.

b) Stability of PTC124-AMP. The stability of PTC124-AMP was assessed under conditions previously described for a cell-free translation system (9) except that 293H cells were used to prepare the lysate. Synthetic *LUC* mRNA containing a PTC at position 190 was prepared using the MegaScript® *in vitro* transcription kit (Ambion, Austin, TX). The reaction mixtures (20 µl) contained 16.5 mM HEPES (KOH) pH 7.4, 85 mM potassium acetate, 1.48 mM magnesium acetate, 0.56 mM ATP, 0.075 mM GTP, 18.75 mM creatine phosphate (di-Tris), 1.275 mM dithiothreitol (DTT), amino acids, creatine kinase, cell extract (60% of the reaction volume), 100 ng RNA, and 0.25% DMSO. Stock solutions of PTC124 (ataluren) and PTC124-AMP were prepared in 100% DMSO and PTC124-AMP at a final concentration of 5uM was added to the *in vitro* reaction. At various

time points following the addition of PTC124-AMP, aliquots were removed and the levels of PTC124-AMP and PTC124 (ataluren) were determined by LC/MS-MS.

Supplementary references

1. Roy B, Leszyk JD, Mangus DA, & Jacobson A (2015) Nonsense suppression by near cognate tRNAs employs alternative base-pairing at codon positions 1 and 3. *Proc. Natl. Acad. Sci. USA* 112:3038-3043.
2. Lentini L*, et al.* (2014) Toward a Rationale for the PTC124 (Ataluren) Promoted Readthrough of Premature Stop Codons: A Computational Approach and GFP-Reporter Cell-Based Assay. *Mol. Pharm.* 11:653-664.
3. Letzring DP, Wolf AS, Brule CE, & Grayhack EJ (2013) Translation of CGA codon repeats in yeast involves quality control components and ribosomal protein L1. *RNA* 19(9):1208-1217.
4. Johansson MJ & Bystrom AS (2004) The Saccharomyces cerevisiae TAN1 gene is required for N4-acetylcytidine formation in tRNA. *RNA* 10(4):712-7199.
5. Belle A, Tanay A, Bitincka L, Shamir R, & O'Shea EK (2006) Quantification of protein half-lives in the budding yeast proteome. *Proc. Natl. Acad. Sci. USA* 103(35):13004-13009.
6. Xue X*, et al.* (2014) Synthetic aminoglycosides efficiently suppress cystic fibrosis transmembrane conductance regulator nonsense mutations and are enhanced by ivacaftor. *Am. J. Respir. Cell Mol. Biol.* 50(4):805-816.
7. Ludwig MR*, et al.* (2016) Surveying the serologic proteome in a tissue-specific kras(G12D) knockin mouse model of pancreatic cancer. *Proteomics* 16(3):516-531.
8. Auld DS*, et al.* (2010) Molecular basis for the high-affinity binding and stabilization of firefly luciferase by PTC124. *Proc. Natl. Acad. Sci. USA* 107(11):4878-4883.
9. Welch EM*, et al.* (2007) PTC124 targets genetic disorders caused by nonsense mutations. *Nature* 447(7140):87-91.

Supplementary figure legends

Fig. S1. Key features of reporter genes expressed in yeast and mammalian cells. (*A*) The yeast *HA-HIS3$_{(UAA100)}$-SF* reporter contained an in-frame 3X HA tag at the N-terminus of its ORF, adjacent StrepII and FLAG (SF) tags at the ORF C-terminus. (*B*) The NanoLuc reporter for mammalian cells that encoded a UGA stop codon at ORF position 12 (W12X). (*C*) The construction of four distinct yeast *LUC* alleles, one wild-type and three with each of the possible PTCs inserted at codon 20 of the *LUC* ORF, was described previously (1). The *HA-LUC$_{(PTC20)}$-SF* reporter set for expression in 293H cells was similar to that used in yeast (1), but contained an intron insertion (site denoted in figure). (*D*) The Turbo GFP-*CFTR*-G542X reporter used to identify amino acids inserted at the PTC during readthrough. The *CFTR* context included in the construct is shown. (*E*) The H2B-GFP reporter originally described by Lentini et al. (2). (*F*) The p53 reporters used to detect ataluren-mediated readthrough encode the p53 ORF with UGA at codons 196 or 213.

Fig. S2. Nonsense-containing reporter transcripts are substrates for NMD. Northern analyses of the *(A) HA-LUC$_{(PTC20)}$-SF* and *(B) HA-HIS3$_{(UAA100)}$-SF* mRNAs expressed in wild-type [*PSI*-] yeast cells without/with drug treatment and in *upf1Δ* cells (as a control). Blots were re-probed for *CYH2* transcripts as an internal NMD control. *SCR1* RNA was used as a loading control. *(C)* RT-qPCR analyses of *HA-LUC-SF* wild-type and nonsense-containing mRNAs in 293H cells after cycloheximide treatment, showing drug-dependent stabilization of the transcripts derived from PTC alleles.

Fig. S3. Readthrough efficiencies of different reporters expressed in mammalian cells. (*A*) Ataluren and G418 increase readthrough of the p53-UGA-196 allele in CALU-6 cells and the p53-UGA-213 allele in HDQ cells. The respective reporters are shown in Fig. S1 and the data depict fold increase over DMSO as quantified by MSD/ELISA (n=3). (*B*) Ataluren and G418 increase readthrough from the H2B-GFP-UGA$_{58}$ reporter depicted in Fig. S1. Western blot of readthrough products in transiently transfected 293H cells. H2B-GFP is the full-length product expressed from a construct lacking a PTC. (*C*) Readthrough efficiency measured as luciferase activity from HA-*LUC*-SF and HA-

LUC$_{(PTC20)}$-SF reporters expressed in 293H cells (n=3; error bars represent standard deviation from the mean). (*D*) Western analyses showing full-length readthrough products expressed from HA-*LUC*$_{(UGA20)}$-SF reporters after ataluren or G418 treatment of 293H cells.

Fig. S4. Ataluren treatment of yeast cells promotes readthrough of HA-*LUC*$_{(PTC20)}$-SF reporter mRNA. Western analyses showing full-length readthrough products expressed from HA-*LUC*$_{(UGA20)}$-SF reporters after ataluren or G418 treatment.

Fig. S5. Half-life of the His3 protein.

Top: representative western blot depicting decay of the WT His3 protein after cycloheximide treatment of yeast cells at t=0. Bar graphs: upper and middle panels depict quantitation of results from untreated and cycloheximide-treated cultures expressing wild-type His3 protein; lower panel depicts quantitation of full-length His3 protein derived from ataluren-mediated readthrough after cycloheximide treatment of yeast cells at t=0. The levels of wild-type or PTC readthrough His3 protein were determined by western blotting and normalized to levels of the Pgk1 protein also determined by western blotting in the same experiments. T15, 30, 45, 60=15, 30, 45, and 60 min after cycloheximide addition.

Fig. S6. PTC124-AMP is rapidly converted to the active readthrough molecule PTC124 (ataluren) in an *in vitro* translation extract. PTC124-AMP at a final concentration of 5uM was added to an *in vitro* readthrough assay. At various time points following the addition of PTC124-AMP (dissolved in DMSO), aliquots were removed and the levels of PTC124-AMP and PTC124 (ataluren) were determined by LC/MS-MS.

Fig. S7. Purification of luciferase readthrough products.

(A) Western blot analysis of the full-length readthrough products purified on Strep-Tactin resin from wild-type [*PSI-*] yeast cells after treatment with ataluren. Anti-FLAG antibody was used for detection. Ec depicts elution fractions (E3-E7) that were pooled and concentrated. *(B)* Silver-stained SDS/PAGE gel showing the results of FLAG - HA

purification of the luciferase readthrough protein (marked with an asterisk) from ataluren-treated 293H cells expressing the HA-*LUC*$_{(UGA20)}$-SF reporter.

Fig. S8. Ataluren-induced His3 and luciferase readthrough products are functional. *(A)* Growth of wild-type cells expressing the HA-*HIS3*$_{(UAA100)}$-SF allele in media lacking histidine with or without drug treatment. *(B)* Luciferase activity from HA-*LUC*-SF reporter with missense mutations introduced at position 20 of luciferase. Luciferase activity is expressed as relative luciferase units/µg of protein (n=3; error bars represent standard deviation from the mean).

Fig. S9. Representative mass spectrometry spectra in CFTR G542WT and G542X samples. Tandem MS2 spectra are illustrated for the CFTR wild-type tryptic peptides and those from three CFTR mutants analyzed in our study; *(A)* G542G; *(B)* G542R; *(C)* G542W; and *(D)* G542C.

Fig. S10. tRNA overexpression analyses. *(A)* Northern analyses of total RNA isolated under acidic conditions from wild-type cells and cells overexpressing tRNA-Arg-UCU or tRNA-Arg-UCG. After polyacrylamide gel electrophoresis and transfer, blots were probed for tRNA-Arg using a ^{32}P-labeled oligonucleotide. The blots were re-probed for tRNA-Glu as a control for equal loading. Lane 1: Wild-type; Lane 2: Wild-type + HA-*LUC*$_{(UGA20)}$-SF; Lane 3: Wild-type + HA-*LUC*$_{(UGA20)}$-SF + tRNA-Arg-UCU; Lane 4: Wild-type + HA-*LUC*$_{(UGA20)}$-SF + tRNA-Arg-UCG. *(B)* Readthrough efficiency measured as luciferase activity from the HA-*LUC*$_{(UGA20)}$-SF reporter from wild-type [*PSI*-] cells or cells overexpressing either tRNA-Arg-UCU or tRNA-Arg-UCG. Luciferase activity is expressed as relative luciferase units/µg of protein/RNA units (n=3; error bars represent standard deviation from the mean). Lane 1: Wild-type + HA-*LUC*$_{(UGA20)}$-SF; Lane 2: Wild-type + HA-*LUC*$_{(UGA20)}$-SF + tRNA-Arg-UCU; Lane 3: Wild-type + HA-*LUC*$_{(UGA20)}$-SF + tRNA-Arg-UCG; Lane 4: Wild-type + HA-*LUC*-SF**.** (*C*) Comparison of amino acid insertion at UGA during termination readthrough of HA-*LUC*$_{(UGA20)}$-SF reporter in yeast cells with either endogenous levels tRNA-Arg-UCU, or overexpression of tRNA-Arg-UCU or tRNA-Arg-UCG. HA-Luc$_{(PTC20)}$-SF proteins purified from yeast cells were subjected to mass

spectrometry analyses. The numbers denote the frequency (± standard deviation of the mean) of insertion of the amino acids at UGA (n=3). The type and the position of mispairing in the codon are depicted for each amino acid inserted. *(D)* Northern blot analyses of total RNA isolated under acidic conditions from wild-type yeast cells and cells overexpressing tRNA-Glu-UUC. After polyacrylamide gel electrophoresis and transfer, blots were probed for tRNA-Glu using a ^{32}P-labeled oligonucleotide. The blots were re-probed for tRNA-Arg-UCU as a control for equal loading. Lanes 1-3 were all derived from the same gel. *(E)* Readthrough efficiency measured as luciferase activity from the HA-*LUC*$_{(UAA20)}$-SF reporter in wild-type yeast cells and cells overexpressing tRNA-Glu-UUC. Luciferase activity is expressed as relative luciferase units/µg of protein/RNA units (n=3; error bars represent standard deviation from the mean*). (F)* Amino acids inserted at UAA during termination readthrough in yeast cells overexpressing tRNA-Glu-UUC. HA-*LUC*$_{(UAA20)}$-SF protein products were purified and subjected to mass spectrometry analyses. The numbers denote the average frequency of insertion of the amino acids at UAA (from two independent experiments).

Supplementary Figure 1

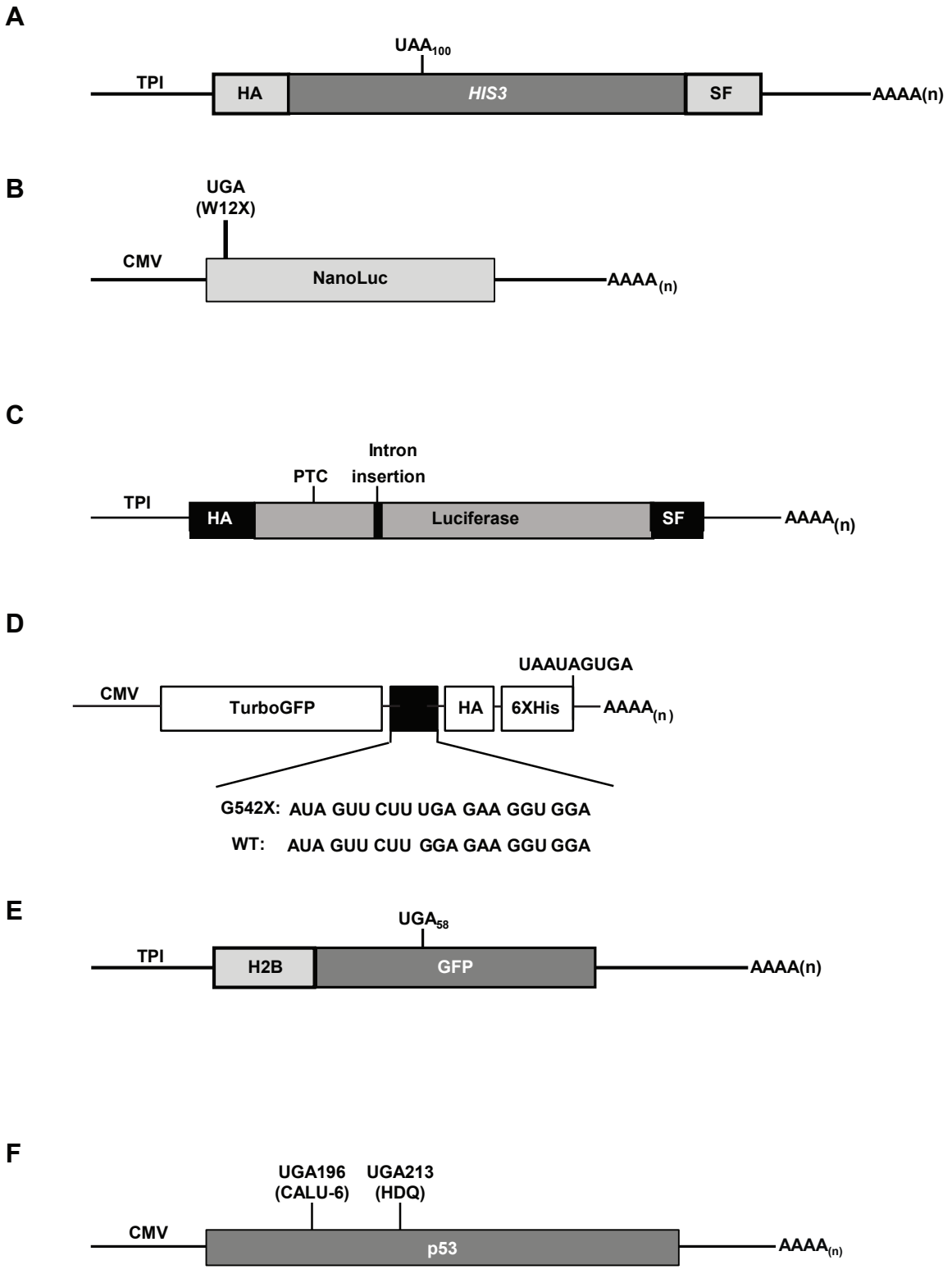

Supplementary Figure 2

A

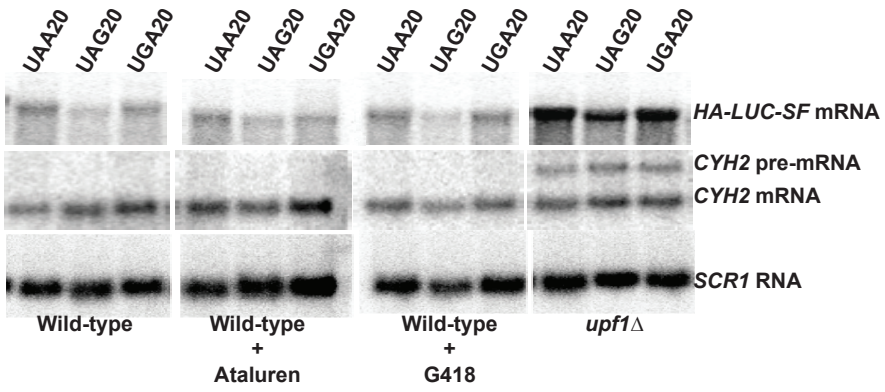

B

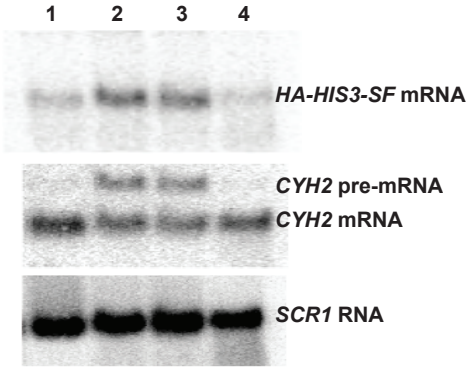

1. Wild-type + HA-HIS3(UAA100)-SF
2. *upf1*Δ + HA-HIS3(UAA100)-SF
3. *upf1*Δ + HA-HIS3(UAA100)-SF + Ataluren
4. Wild-type + HA-HIS3(UAA100)-SF + Ataluren

C

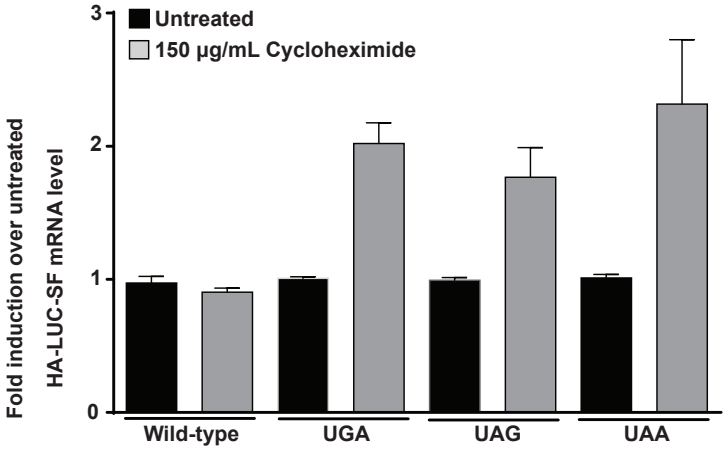

Supplementary Figure 3

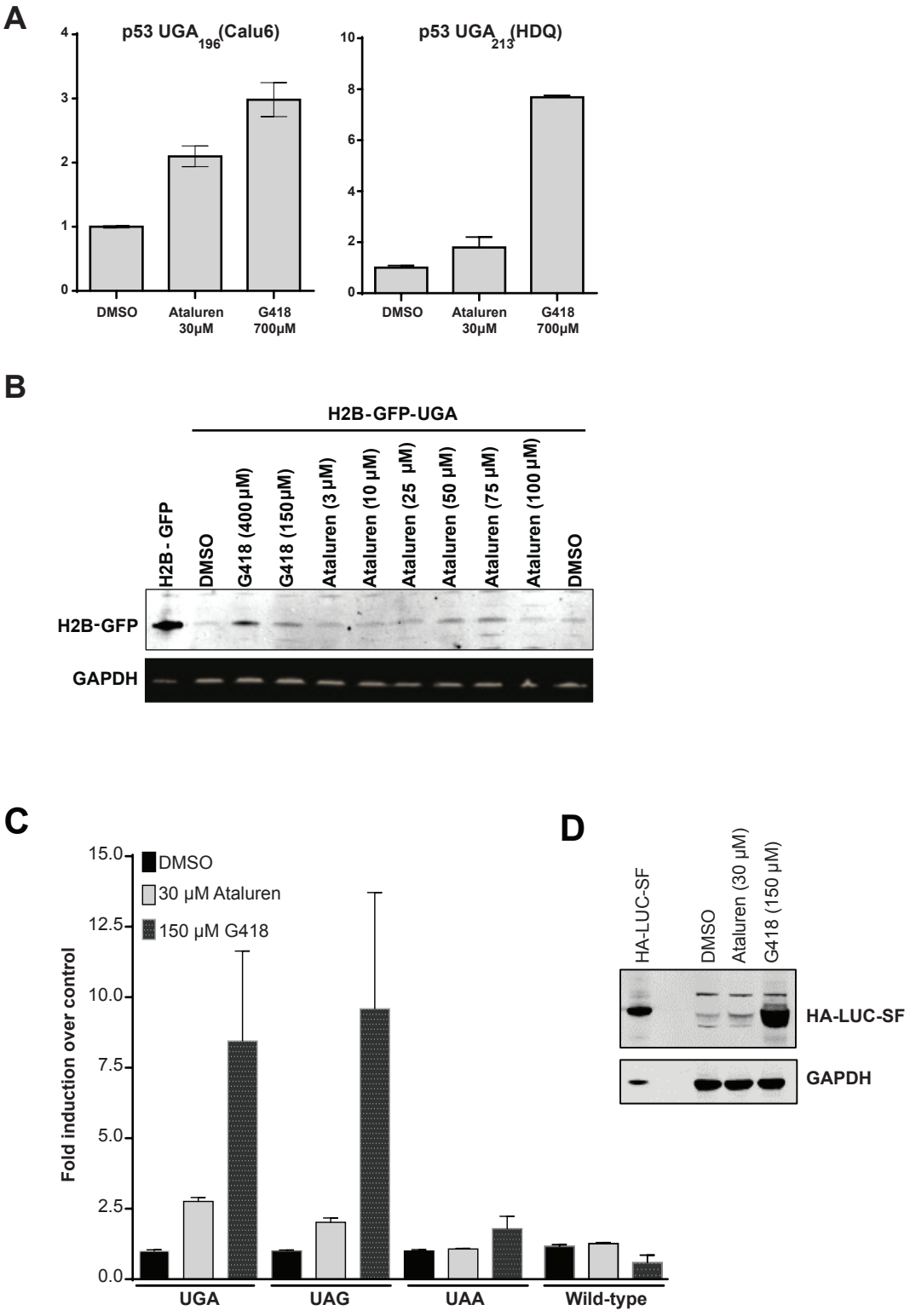

Supplementary Figure 4

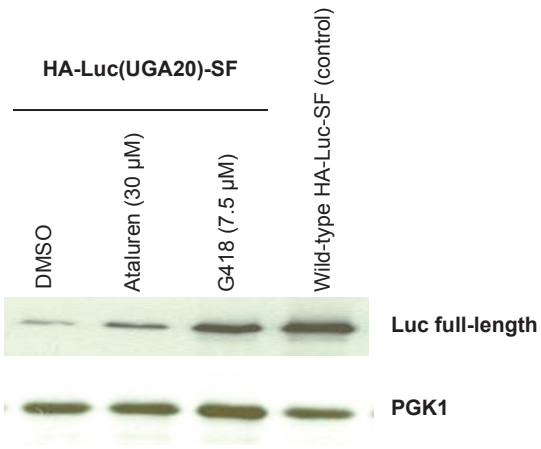

Supplementary Figure 5

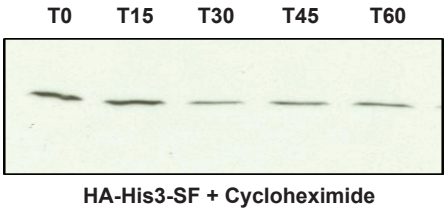

HA-His3-SF + Cycloheximide

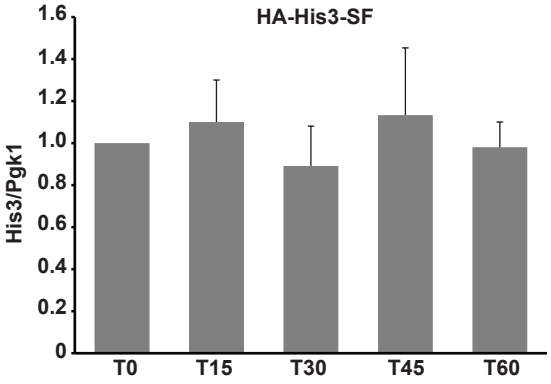

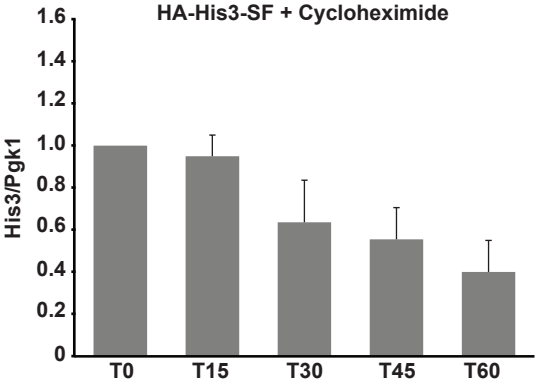

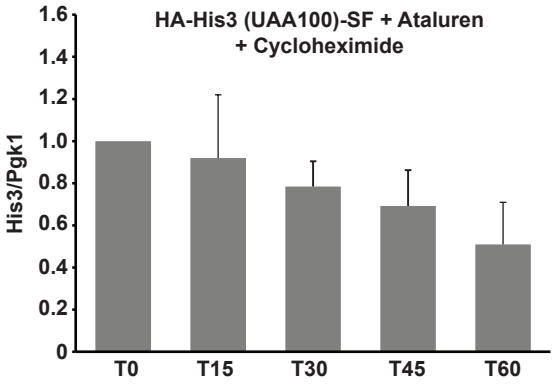

Supplementary Figure 6

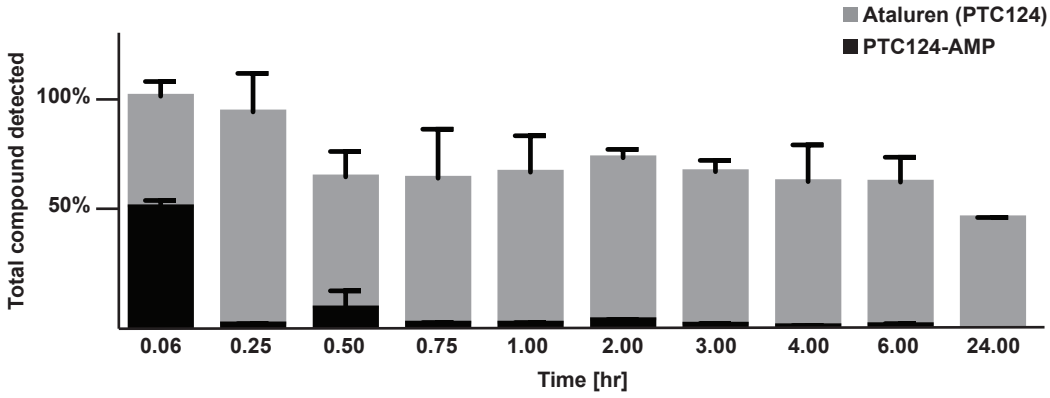

Supplementary Figure 7

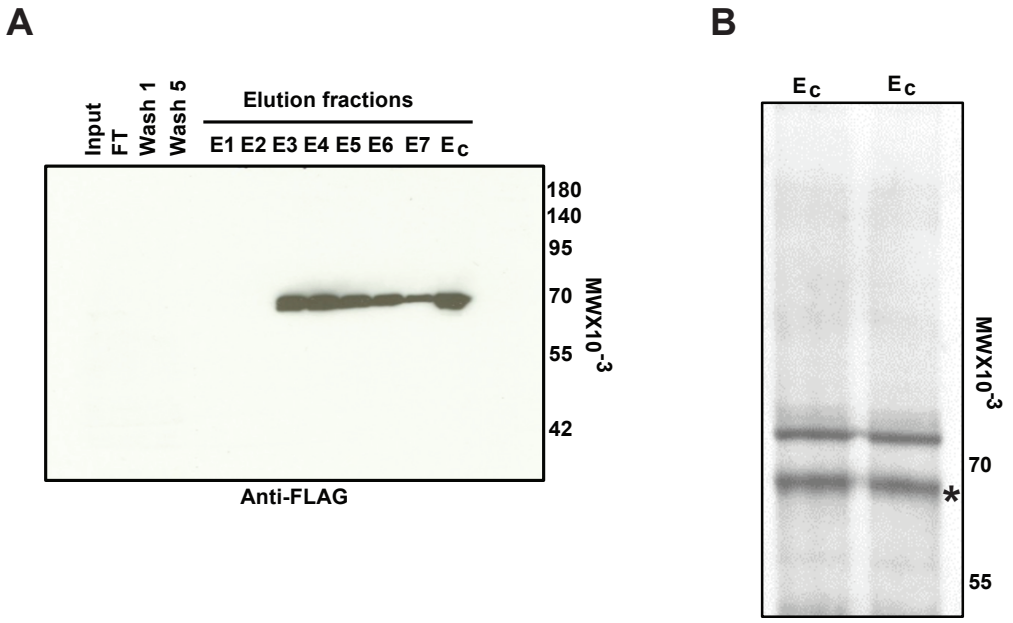

Supplementary Figure 8

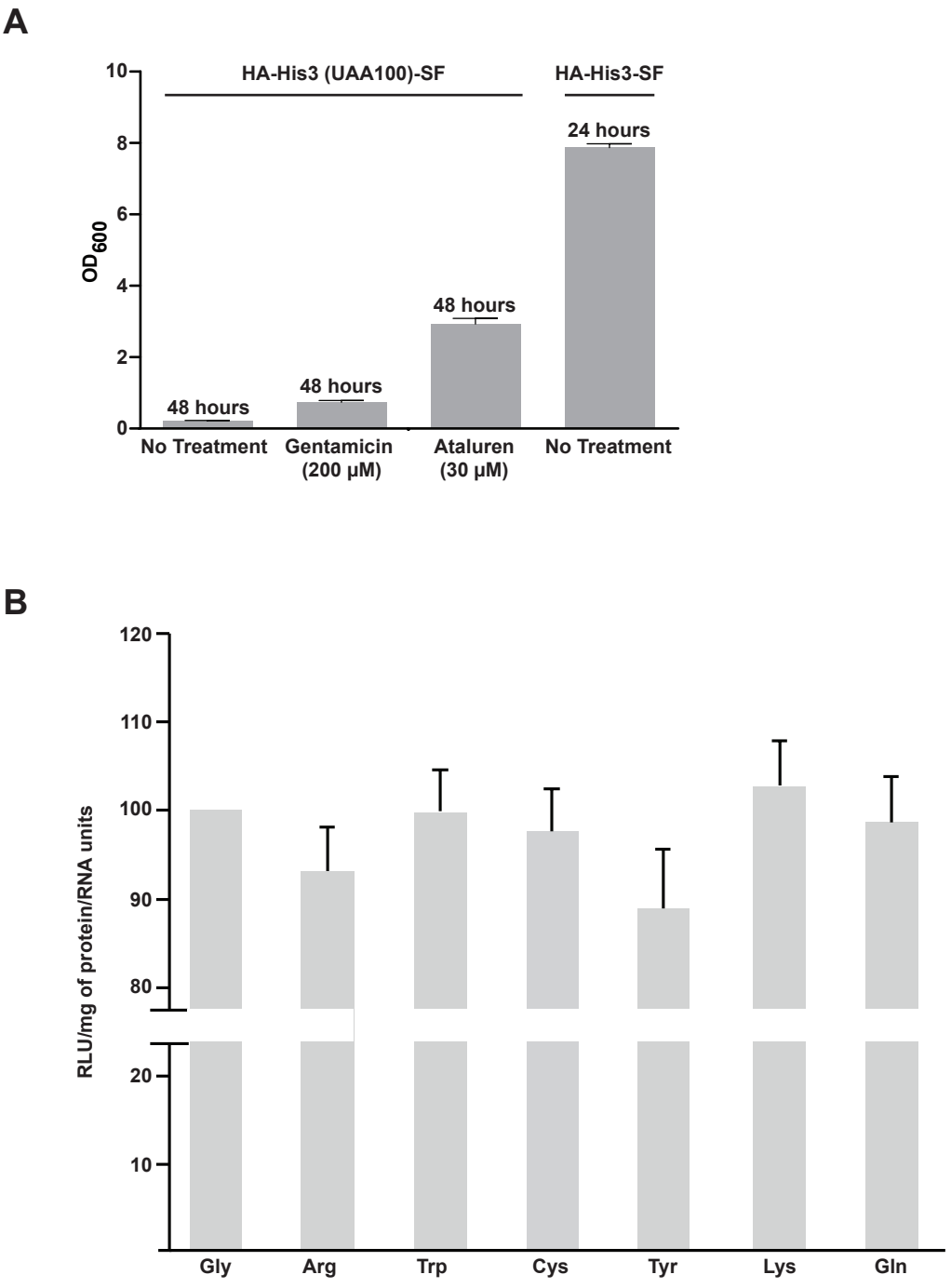

Supplementary Figure 9

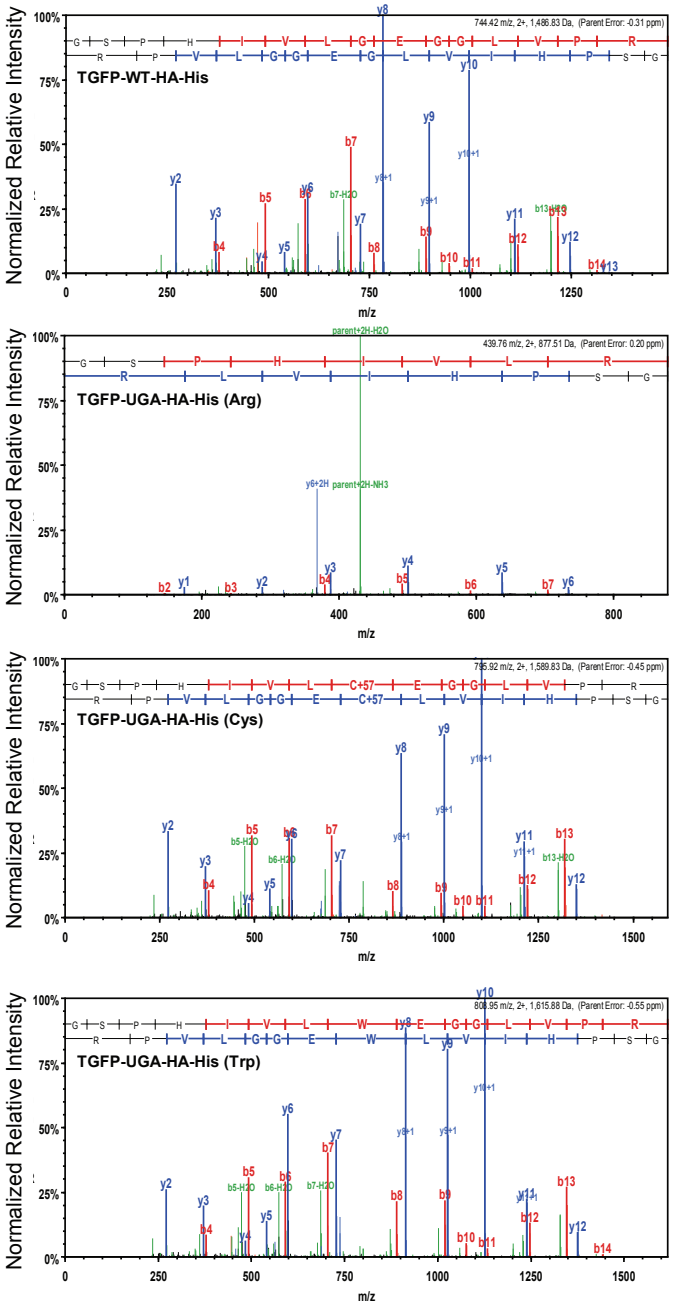

Supplementary Figure 10

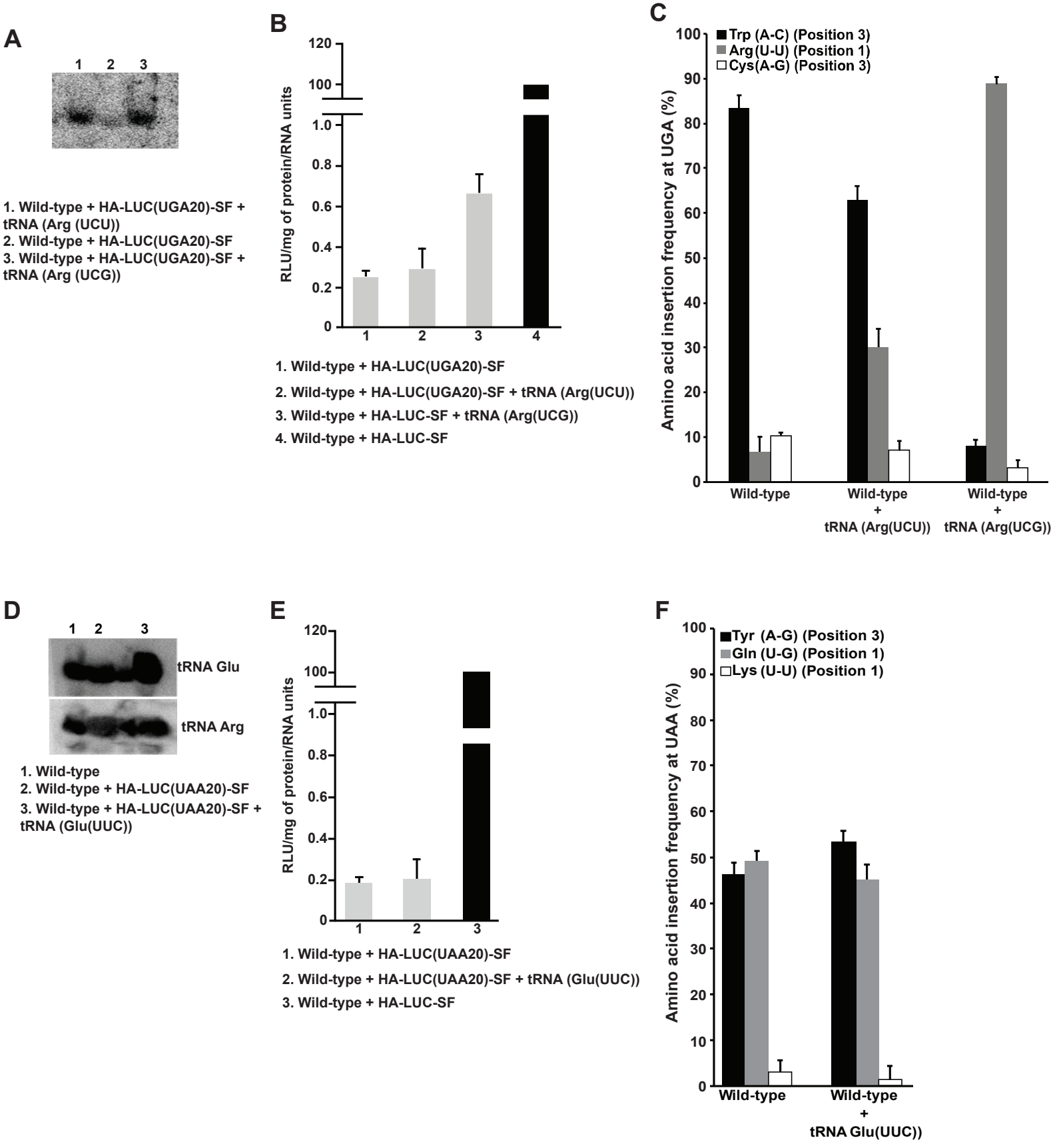

Table S1. Amino acids inserted at PTCs after treatment of wild-type [*PSI-*] yeast cells with 7.5 µM G418.

Codon	Amino acid inserted	Frequency of insertion (%)		Mispairing event
		Experiment 1	Experiment 2	
UAA	Tyr	51.1	52.6	Position 3 (A-G)
	Gln	46.9	45.4	Position 1 (U-G)
	Lys	1.1	2.0	Position 1(U-U)
UAG	Tyr	1.59	1.55	Position 3 (G-G)
	Gln	4.35	5.1	Position 1 (U-G)
	Lys	90.9	90.8	Position 1(U-U)
	Trp	1.55	0.85	Position 2 (A-C)
	Arg	0.87	0.79	Non-cognate tRNA employing position 1 (U-G) and position 2 (A-C) mispairing
	Cys	0.26	0.18	Non-cognate tRNA employing position 2 (A-C) position 3 (G-A/G-G) mispairing
	Ser	0.02	0.02	Position 2 (A-G); Non-cognate tRNA employing position 2 (A-G) and position 3 (G-A/G-G/G-U) mispairing
	Gly	0.18	0.53	Non-cognate tRNA employing position 1(U-C) and position 2 (A-C) mispairing
	Glu	0.03	0.03	Position 1 (U-C); Non-cognate tRNA employing position 1 (U-C) and position 3 (G-U) mispairing
	Thr	0.11	0.08	Non-cognate tRNA employing position 1(U-U) and position 2 (A-G) mispairing
	Phe	0.02	0	Non-cognate tRNA employing position 2(A-A) and position 3 (G-A/G-G) mispairing
	Val	0	0.02	Non-cognate tRNA employing position 1(U-C) and position 2 (A-A) mispairing
UGA	Trp	61.0	57.3	Position 3 (A-C)
	Arg	11.0	16.2	Position 1 (U-U)
	Cys	27.9	26.5	Position 3 (A-G)

Table S2. Amino acids inserted at PTCs after treatment of wild-type [*PSI-*] yeast cells with 15 µMG418.

Codon	Amino acid inserted	Frequency of insertion (%)	Mispairing event
UAA	Tyr	72.9	Position 3 (A-G)
	Gln	24.2	Position 1 (U-G)
	Lys	2.5	Position 1(U-U)
	His	0.16	Non-cognate tRNA employing position 1 (U-G) and position 2 (A-A/A-G) mispairing
	Trp	0.11	Non-cognate tRNA employing position 1 and 2 (A-C) mispairing
UAG	Tyr	2.25	Position 3 (G-G)
	Gln	4.36	Position 1 (U-G)
	Lys	90.5	Position 1(U-U)
	Trp	0.98	Position 2 (A-C)
	Arg	0.81	Non-cognate tRNA employing position 1 (U-G) and position 2 (A-C) mispairing
	Cys	0.39	Non-cognate tRNA employing position 2 (A-C) and position 3 (G-G/G-A) mispairing
	Ser	0.05	Position 2 (A-G); Non-cognate tRNA employing position 2 (A-G) and position 3 (G-A/G-G/G-U) mispairing
	Gly	0.42	Non-cognate tRNA employing position 1(U-C) and position 2 (A-C) mispairing
	Glu	0.02	Position 1 (U-C); Non-cognate tRNA employing position 1 (U-C) and position 3 (G-U) mispairing
	Thr	0.15	Non-cognate tRNA employing position 1(U-U) and position 2 (A-G) mispairing
	Val	0.02	Non-cognate tRNA employing position 1(U-C) and position 2 (A-A) mispairing
UGA	Trp	47.9	Position 3 (A-C)
	Arg	26.1	Position 1 (U-U)
	Cys	24.4	Position 3 (A-G)
	Tyr	0.81	Non-cognate tRNA employing position 2 (G-U) and position 3 (A-A/A-G) mispairing
	Lys	0.56	Non-cognate tRNA employing position 1 (U-U) and position 2 (G-U) mispairing

Table S3. Possible codon-anticodon base pairings during PTC readthrough.

Codon Position	Mispaired tRNA sequence (3'-5')	AA encoded	BP created
1 UAA	UUU	Lys	U-U
	UUG	Gln	U-G
	UUC	Glu	U-C
	UUA	STOP	U-A
2 UAA	UUA	STOP	A-U
	UGA	Ser	A-G
	UCA	STOP	A-C
	UAA	Leu	A-A
3 UAA	UUA	Stop	A-U
	GUA	Tyr	A-G
	AUA		A-A
	CUA	Stop	A-C

Codon Position	Mispaired tRNA sequence (5-3')	AA encoded	BP created
1 UAG	CUU	Lys	U-U
	CUG	Gln	U-G
	CUC	Glu	U-C
	CUA	STOP	U-A
2 UAG	CUA	STOP	A-U
	CGA	Ser	A-G
	CCA	Trp	A-C
	CAA	Leu	A-A
3 UAG	UUA	STOP	G-U
	GUA	Tyr	G-G
	AUA		G-A
	CUA	Stop	G-C

Codon Position	Mispaired tRNA sequence (5'-3')	AA encoded	BP created
1 UGA	UCU	Arg	U-U
	UCG		U-G
	UCC	Gly	U-C
	UCA	Stop	U-A
2 UGA	UUA	Stop	G-U
	UGA	Ser	G-G
	UCA	Stop	G-C
	UAA	Leu	G-A
1 UGA	UCA	Stop	A-U
	GCA	Cys	A-G
	ACA		A-A
	CCA	Trp	A-C

Table S4. Amino acids inserted at UGA after treatment of HEK293cells with Gentamicin.

Codon Position	Mispaired tRNA sequence (5'-3')	AA encoded	BP created	Gentamicin (average ± stdev)
1 UGA	UCU	Arg	U-U	48.4±6.8
	UCG		U-G	
	UCC	Gly	U-C	
	UCA	Stop	U-A	
2 UGA	UUA	Stop	G-U	
	UGA	Ser	G-G	
	UCA	Stop	G-C	
	UAA	Leu	G-A	
1 UGA	UCA	Stop	A-U	
	GCA	Cys	A-G	27.0±9.8
	ACA		A-A	
	CCA	Trp	A-C	24.2±3

Table S5. Amino acids inserted at G542X after treatment of HEK293 cells with G418

Sample	Peptide Sequence	m/z (z, ppm)	RT (min)	R-NSC Exp 1	R-NSC Exp 2	Ave R-NSC
WT	GSPHIVLGEGGLVPR	496.62 (3, -0.36)	66.5	100	100	100
G542X	GSPHIVLR	439.76 (2, 0.20)	41.2	26	15	20
	GSPHIVLCEGGLVPR (IAA modified)	530.95 (3, -0.15)	67.4	41	46	44
	GSPHIVLWEGGLVPR	539.64 (3, 0.16)	81.9	33	38	36

Table S6. Amino acids inserted at PTCs after treatment of 293H cells with ataluren or G418.

Codon Position	Mispaired tRNA sequence (3'-5')	AA encoded	BP created	DMSO	DMSO	DMSO	Ataluren	Ataluren	Ataluren	G418	G418	G418	DMSO average ± stdev	Ataluren average ± stdev	G418 average ± stdev
1 UAA	UUU	Lys	U-U												
	UUG	Gln	U-G	23.4	32.6	41.2	39.2	51.9	28.6	37	53.6	65.3	32.4 ± 8.9	39.9 ± 11.7	52 ± 14.2
	UUC	Glu	U-C												
	UUA	STOP	U-A												
2 UAA	UUA	STOP	A-U												
	UGA	Ser	A-G												
	UCA	STOP	A-C												
	UAA	Leu	A-A												
3 UAA	UUA	Stop	A-U												
	GUA	Tyr	A-G	76.5	67.3	58.7	59.9	45.7	68.1	62.7	46.4	34.6	67.5 ± 8.9	57.9 ± 11.3	47.9 ± 14.1
	AUA		A-A												
	CUA	Stop	A-C												

Codon Position	Mispaired tRNA sequence (5-3')	AA encoded	BP created	DMSO	DMSO	DMSO	DMSO	Ataluren	Ataluren	Ataluren	Ataluren	Ataluren	Ataluren	G418	G418	G418	G418	DMSO average ± stdev	Ataluren average ± stdev	G418 average ± stdev
1 UAG	CUU	Lys	U-U											3	1.1	1.5	2.2			2.0 ± 0.8
	CUG	Gln	U-G	34.9	39	15	11.9	81.4	33.7	30.2	81.4	45.1	47.3	80	97.7	87.9	80.5	25.2 ± 13.7	53.2 ± 20.3	86.5 ± 8.3
	CUC	Glu	U-C																	
	CUA	STOP	U-A																	
2 UAG	CUA	STOP	A-U																	
	CGA	Ser	A-G																	
	CCA	Trp	A-C	2.4	2.6		0.19	2.1	0.49	0.2	1.7	4.9	1.2					1.3 ± 1.4	1.8 ± 1.9	
	CAA	Leu	A-A																	
3 UAG	UUA	STOP	G-U																	
	GUA	Tyr	G-G	61.6	58.8	84	87.8	15.6	64.2	69.3	15.7	48.9	49.9	16	1.1	10.1	16	73.1 ± 15.0	43.9 ± 20.9	10.8 ± 7.0
	AUA		G-A																	
	CUA	Stop	G-C																	

Codon Position	Mispaired tRNA sequence (5'-3')	AA encoded	BP created	DMSO	DMSO	DMSO	Ataluren	Ataluren	Ataluren	Ataluren	Ataluren	G418	G418	G418	G418	DMSO average ± stdev	Ataluren average ± stdev	G418 average ± stdev
1 UGA	UCU	Arg	U-U	56	60.5	59.24	63.7	65.3	57.5	86	76	51.7	66.7	79.7	60	58.6 ± 2.3	69.7 ±11.3	64.5 ± 11.8
	UCG		U-G															
	UCC	Gly	U-C															
	UCA	Stop	U-A															
2 UGA	UUA	Stop	G-U															
	UGA	Ser	G-G															
	UCA	Stop	G-C															
	UAA	Leu	G-A															
1 UGA	UCA	Stop	A-U															
	GCA	Cys	A-G				0.5	0.5	2	0.06	0.2	28.8	11.2	12.4	18.3		0.7 ± 0.78	17.7 ± 8.0
	ACA		A-A															
	CCA	Trp	A-C	44	39.5	40.76	35.7	34.2	40.2	13	21	19.5	22.1	7.8	22	41.4 ± 2.3	28.8 ± 11.4	17.9 ± 6.8

Table S7. Oligonucleotides used in this study.

Position 20 Arg For	CTACCCACTCGAAGACAGAACCGCCGGCGAGCAG
Position 20 Arg Rev	CTGCTCGCCGGCGGTTCTGTCTTCGAGTGGGTAG
Position 20 Trp For	CTACCCACTCGAAGACTGGACCGCCGGCGAGCAG
Position 20 Trp Rev	CTGCTCGCCGGCGGTCCAGTCTTCGAGTGGGTAG
Position 20 Cys For	CTACCCACTCGAAGACTGCACCGCCGGCGAGCAG
Position 20 Cys Rev	CTGCTCGCCGGCGGTGCAGTCTTCGAGTGGGTAG
Position 20 Tyr For	CTACCCACTCGAAGACTACACCGCCGGCGAGCAG
Position 20 Tyr Rev	CTGCTCGCCGGCGGTGTAGTCTTCGAGTGGGTAG
Position 20 Lys For	CTACCCACTCGAAGACAAAACCGCCGGCGAGCAG
Position 20 Lys Rev	CTGCTCGCCGGCGGTTTTGTCTTCGAGTGGGTAG
Position 20 Gln For	CTACCCACTCGAAGACCAAACCGCCGGCGAGCAG
Position 20 Gln Rev	CTGCTCGCCGGCGGTTTGGTCTTCGAGTGGGTAG
DB4084	CGTTGGGGACTGACGACAGACAGCC
DB4085	GGCTGTCTGTCGTCAGTCCCCAACG

For= Forward primer
Rev= Reverse primer